The quasinormal modes of non-rotating black holes and wormholes

by

Vadim Smirnov

B.Sc., Moscow Institute of Physics and Technology, 2019

Thesis Submitted in Partial Fulfillment of the
Requirements for the Degree of
Master of Science

in the
Department of Physics
Faculty of Science

SIMON FRASER UNIVERSITY
Summer 2022

Declaration of Committee

Name:	**Vadim Smirnov**
Degree:	**Master of Science (Physics)**
Thesis title:	**The quasinormal modes of non-rotating black holes and wormholes**
Committee:	**Chair:** Malcolm Kennett Associate Professor, Physics
	Andrei Frolov Supervisor Associate Professor, Physics
	Levon Pogosian Committee Member Professor, Physics
	Gabor Kunstatter Examiner Adjunct Professor, Physics

Abstract

At the beginning of the last century, solutions to the Einstein equation indicated the existence of mysterious objects, later called black holes. The Schwarzschild metric describes the geometry of the space-time of a black hole with the presence of two singularities. One of them is called the event horizon, in the vicinity of which gravity is extreme, which leaves the question of the truth of the Schwarzschild geometry open. Direct and indirect observations, such as the study of quasi-normal modes, are likely to be the most valuable for studying the structure of a black hole.

Quasi-normal modes are the response to the perturbation of the geometry of a black hole. The mathematical structure of such modes is quite nontrivial, and these are complex functions oscillating at a "frequency" that is a complex number. The real part is the oscillation frequency while the imaginary gives the rate at which oscillations are damped.

A more mysterious object that may exist in the universe is a wormhole, geometrically outwardly imitating a black hole. This fact may cause some inaccuracy when observing an astrophysical object. Comparing the perturbation profiles of these objects allows us to see that the quasi-normal modes of a black hole obey the characteristic ringdown signal. At the same time, for a wormhole, it theoretically turns out that the quasi-normal modes are a series of echoes representing a periodically repeating signal.

Keywords: Black Hole; Wormhole; quasinormal modes; Schwarzschild geometry; Linearized perturbation theory

Dedication

I dedicate this thesis to my wife, Alia, my parents and grandparents.

Acknowledgements

I would like to thank my supervisor, Andrei Frolov, for his accurate guidance, support, and time provided throughout my study resulted in fruitful research. Furthermore, I am grateful to Levon Pogosian for contributing to my research and support in hard times. It was a great honour for me to give talks at the seminars organized by Levon. I would like to say a special big thank you to my internal examiner Gabor Kunstatter, who thoroughly read my thesis and made several vital remarks and comments.

I want to express my great gratitude to Hamidreza Mirpooryan, Ali Nezhadsafavi, Zhuangfei Wang, Guillermo Quispe, Jonathan Barenboim, Alexei Bunevich and Hamza Hanif for their kind words of support while my study at SFU.

I have a debt of gratitude to pay to Andrew DeBenedictis and Kero Lau, who devoted a lot of time to personal conversations during the study course. Also, I would like to thank Michael D. Green and Ramin G. Daghigh from the Physics department at Metropolitan State University for their contribution. Finally, I am obliged to Daniel Seyed Mahmoud, who, with great joy, agreed to make grammatical corrections to the thesis.

Table of Contents

List of Tables

List of Figures

Chapter 1

Introduction

One of the most unusual and mysterious predictions of the last century was the expected existence of black holes in the Universe. In 1915, one month after Einstein's publication "The Field Equations of Gravitation" [16], Karl Schwarzschild derived a non-trivial solution for the Einstein field equations concerning a stationary, isolated mass in four-dimensional space-time, known as the Schwarzschild Black Hole (BH) [36].

In 2016, one hundred years after K. Schwarzschild's paper, Physical Review Letters journal published an article on the detection of gravitational waves by the Laser Interferometer Gravitational-Wave Observatory (LIGO) [1]. The article presented two significant scientific events. Firstly, Gravitational Waves (GW) were detected by physical sensors, which agreed with the theoretical predictions of Albert Einstein's General Relativity (GR). And secondly, the LIGO observed two BHs merging for the first time since John A. Wheeler pronounced the words "Black hole" in 1968. These events have started a new era of GW astronomy.

The emitted GWs from merging BHs can be separated into three distinct phases [1]. Initially, as both BHs attract and experience multiple rotations,i.e. they are orbiting around each other and infall to a common centre of attraction. This results in a quasi-periodic oscillation of increasing frequency. Next, there is a short burst as both BHs merge into one. Finally, in the third and final stage, like a rung bell, the oscillations of the newly merged BH rapidly attenuate.

This research aims to identify qualitative and quantitative patterns of gravitational waveforms and spectra during the last phase. We approach this by modelling it as a scattering problem of a scalar field on the background of a BH. Additionally, we investigate how a Schwarzschild BH responds to an external gravitational perturbation. An example of a gravitational perturbation is a massive particle, such as a piece of a star falling towards a BH along a geodesic path. Or a scalar field distribution, such as a scalar boson. A perturbed BH generates gravitational waves, which carry essential astrophysical information such as mass, spin, or charge, based on the "no-hair" theorem [28].

A perturbed BH emits a "ringdown" signal as introduced in [10], the oscillations of which are known as quasinormal modes (QNMs), and the associated frequencies as quasinormal

frequencies (QNFs), which are then followed by a power-law decay [33]. The frequencies of oscillations are complex numbers, the real part related to temporal oscillation, and the imaginary being the rate of exponential decay [34].

Finally, we consider the perturbation of Ellis-Bronnikov traversable Worm Holes (WHs) ([17], [3]) and a toy-model of the Schwarzschild-like WH by a massless scalar field [8].

The thesis is structured as follows.

Chapter 2 provides an essential theoretical background for understanding the fundamentals of Schwarzschild BH theory. The chapter begins with the Einstein field equations and a definition of BH geometry as a metric tensor in space-time. Next, we derive the equation of the evolution of a massless scalar field in the Schwarzschild geometry induced by a BH. Followed by Regge and Wheeler's original paper ([34]), we develop a linearized gravitational perturbation theory of a BH and derive all equations needed. The gravitational perturbation is particularly interesting since every metric component can split into either polar or axial parts depending on parity. For this, we set up a boundary condition problem and solve it using Wolfram Mathematica.

Chapter 3 discusses the development of the theory of WHs.

Chapter 4 focuses on extracting QNF spectra using the third order WKB approximation ([35] and [20]) and the continued fraction method (CFM) known as Leaver's method [25]. We begin with discussing boundary conditions (see p.6 [24]) for the master equation obtained in chapter 2 and finish with the physical explanation of the results.

Chapter 5 discusses the WH's response to the massless scalar field perturbation.

In chapter 6, we summarize and conclude with the results and provide some ideas for future prospects.

Chapter 2

Theoretical Background

This chapter will introduce equations, parameters, concepts and notation used throughout our research. We will also give a brief theoretical overview of the Schwarzschild BH. Following convention, we will use the geometrized unit system where the speed of light c in a vacuum and G the Newtonian constant of gravitation are set to be $G = c = 1$.

2.1 Schwarzschild black hole

In 1915, Albert Einstein presented "The Field Equations of Gravitation" [16] to the scientific community. In it, he expresses the local space-time geometry in terms of the Einstein tensor $G_{\mu\nu}$, and the local mass and momentum as sources of a gravitational field represented by an stress-energy tensor $T_{\mu\nu}$. This equation can be derived from the Einstein–Hilbert action S_{E-H} which is

$$S_{E-H} = \frac{1}{2\kappa}\int (R - 2\Lambda)\sqrt{-g}d^4x + S_m, \tag{2.1}$$

where the constant $\kappa = 8\pi$ (in the geometrized units) is called the Einstein gravitational constant. Here S_m is the matter action which describes any type of field (scalar, boson, fermion, etc) and Λ is the cosmological constant which is set to zero in our research. In order to obtain a physical law which governs the nature of processes hidden in the action (2.1), the action principle requires that the variation δS_{E-H} should be zero at any variation of the metric $\delta g^{\mu\nu}$ that vanishes at the boundaries.

This leads to the equality of the Einstein tensor $G_{\mu\nu}$ and stress-energy tensor $T_{\mu\nu}$, and so forms the basis for the study and verification the modern theory of gravity

$$G_{\mu\nu} = R_{\mu\nu} - \frac{1}{2}Rg_{\mu\nu} + \Lambda g_{\mu\nu} = 8\pi T_{\mu\nu}, \tag{2.2}$$

where the indices μ,ν run over the time and spatial coordinates (t, x, y, z) which are usually enumerated as (x^0,x^1,x^2,x^3), $g_{\mu\nu}$ is the metric tensor in curved space which plays a fundamental role in grativational theories and space-time metrics. It is a symmetric (0,2) tensor

with non-vanishing determinant $g = |g_{\mu\nu}|$ therefore we can define the inverse metric $g^{\mu\nu}$ as

$$g^{\mu\nu} g = g_{\alpha b} g^{\alpha\mu} = \delta^{\mu}_{b}. \tag{2.3}$$

The metric's components are dynamic variables which define the geometry of space-time. Namely, the scalar product in four dimensions and therefore the path length is as follows

$$ds^2 = g_{\mu\nu} dx^{\mu} dx^{\nu}. \tag{2.4}$$

According to Einstein's theory of gravity, the general theory of relativity, the four-dimensional space-time is warped due to gravity. Matter as a source of the gravitational field bends the space around itself, and the denser it is, the stronger the curvature.

The stress-energy tensor is defined as

$$T_{\mu\nu} = \frac{2}{\sqrt{-g}} \frac{\delta S_m}{\delta g^{\mu\nu}}. \tag{2.5}$$

In order to continue studying Einstein's equations, an explanation is needed regarding notation and symbols.

Christoffel symbols Γ^{μ} are

$$\Gamma^{\mu}_{\alpha b} = \frac{1}{2} g^{\mu\nu} (g_{b\nu,\alpha} + g_{\nu\alpha,b} - g_{\alpha b,\nu}), \tag{2.6}$$

where each comma denotes the derivative with respect to the coordinate.

The Riemann curvature tensor has components

$$R_{\mu\nu\rho\sigma} = g_{\rho\lambda} (\Gamma^{\lambda}_{\nu\sigma,\mu} - \Gamma^{\lambda}_{\mu\sigma,\nu} + \Gamma^{\lambda}_{\mu\eta} \Gamma^{\eta}_{\nu\sigma} - \Gamma^{\lambda}_{\nu\eta} \Gamma^{\eta}_{\mu\sigma}). \tag{2.7}$$

Then the Ricci tensor in Eq. (2.2) is the symmetric tensor and defined from $R_{\mu\nu\rho\sigma}$ as

$$R_{\mu\nu} = g^{\rho\sigma} R_{\rho\mu\sigma\nu}, \tag{2.8}$$

and the Ricci Scalar is

$$R = g^{\mu\nu} R_{\mu\nu}. \tag{2.9}$$

In order to solve equation (2.2) we need to know the components of the $g_{\mu\nu}$ metric tensor. The first non-trivial exact solution of the vacuum Einstein equations (2.2) was derived by Karl Schwarzschild in 1916 [36]. It describes the gravitational field outside of a BH, a massive static, non-rotating, and spherically symmetric region of space-time. The properties of this solution are incredibly unusual. Firstly, it implies that a black hole does not have a material surface but has a boundary in the void - a sphere of the gravitational radius or Schwarzschild radius r_s. At the edge of a black hole, gravity becomes infinite. The spherical

surface at $r = r_s$, known as the Event Horizon, is a null surface(see pp. 240-241 [9]). Bodies and radiation can enter this sphere, but nothing can exit. A clock (proper time) slows down as seen by an observer at infinity and stops on the surface altogether. Nevertheless, in many cases, this empty boundary behaves like a material surface endowed with specific mechanical, electromagnetic and thermal properties. This solution defines the metric of space-time near the black hole as

$$ds^2 = g_{\mu\nu}dx^\mu dx^\nu = -\left(1 - \frac{r_s}{r}\right)dt^2 + \left(1 - \frac{r_s}{r}\right)^{-1} dr^2 + r^2 d\Omega^2, \tag{2.10}$$

where $d\Omega^2 = d\theta^2 + \sin^2\theta d\varphi^2$ is the standard Riemannian metric on a unit two-sphere with $\theta \in [0, \pi]$ and $\varphi \in [0, 2\pi)$, $r_s = 2GM$ is the Schwarzschild radius, M is a constant which represents the gravitational mass of the BH. At spatial infinity, this metric approaches the Minkowski metric asymptotically.

There are two singularities for r, the Schwarzschild coordinate at zero and at the Schwarzschild radius, therefore, the metric is only defined on the exterior region $r > r_s$. It is not difficult to show that the metric can be analytically extended to singularity(see pp. 222-229 [9]). The singularity at $r = 2MG$ can be removed by setting new coordinates first introduced by Eddington and Finkelstein.

We rewrite the metric (2.10) in the following way

$$ds^2 = g_{\mu\nu}dx^\mu dx^\nu = \left(1 - \frac{r_s}{r}\right)\left(-dt^2 + \frac{dr^2}{\left(1 - \frac{r_s}{r}\right)^2}\right) + r^2 d\Omega^2, \tag{2.11}$$

and then introduce the new coordinate substitution

$$\frac{dr_*}{dr} = \left(1 - \frac{r_s}{r}\right)^{-1}, \tag{2.12}$$

where r_* is called the tortoise coordinate.

The re-written metric will have the following view

$$ds^2 = g_{\mu\nu}dx^\mu dx^\nu = \left(1 - \frac{r_s}{r}\right)\left(-dt^2 + dr_*^2\right) + r^2 d\Omega^2, \tag{2.13}$$

The Eddington–Finkelstein coordinates are obtained by replacing the coordinate t with the new coordinate

$$v = t \pm r_*,$$

and so, the new metric has the form

$$ds^2 = -\left(1 - \frac{r_s}{r}\right)dv^2 \pm 2dvdr + r^2 d\Omega^2. \tag{2.14}$$

The plus and minus sign correspond to the so-called ingoing and outgoing Eddington–Finkelstein (EF) coordinates. Both are explicitly non-singular at the Schwarzschild radius.

Note that there is no possibility of preventing the $r = 0$ singularity by changing coordinate systems. There is a scalar quantity in general relativity which diverges only at $r = 0$ and does not depend on the choice of coordinate system used. This is called the Kretschmann invariant and is given by the formula

$$K \equiv R_{\alpha b \gamma \delta} R^{\alpha b \gamma \delta} = \frac{48M^2}{r^6}, \tag{2.15}$$

which indicates the existence of a gravitational singularity in Schwarzschild space-time due to its infinite curvature.

2.2 Scalar Perturbations

Let us consider a massless scalar field ϕ in the gravitational field created by a BH with the metric (2.10). The equation governing the evolution of ϕ in a curved time-space with background metric $g_{\mu\nu}$ is the massless Klein-Gordon equation (see Ch.12.1 in [27]).

$$\Box\phi = \sqrt{-g}\partial_\mu(\sqrt{-g}g^{\mu\nu}\partial_\nu)\phi = 0, \tag{2.16}$$

where g denotes of the determinant of $g^{\mu\nu}$ and in the explicit form is

$$-\sin\theta\frac{r^2}{f}\frac{\partial\phi^2}{\partial t^2} + \sin\theta\frac{\partial}{\partial r}\left(r^2 f\frac{\partial\phi}{\partial r}\right) + \frac{\partial}{\partial\theta}\left(sin\theta\frac{\partial\phi}{\partial\theta}\right) + \frac{1}{sin^2\varphi}\frac{\partial^2\phi}{\partial\varphi^2} = 0 \tag{2.17}$$

Due to spherical symmetry of the metric, it is useful to expand $\phi(x)$ into the spherical harmonics basis

$$\phi(t, r, \theta, \varphi) = \frac{1}{r}\sum_{l=0}^{\infty}\sum_{m=-l}^{l} u_{lm}(t, r)Y_{lm}(\theta, \varphi). \tag{2.18}$$

By using this expansion in the Klein-Gordon equation (2.3) for the field ϕ, we obtain

$$A\partial_r(A\partial_r u_{lm}) - \partial_t^2 u_{lm} - V_{\text{eff}}(r)u_{lm} = 0, \tag{2.19}$$

where $A(r) = 1 - \dfrac{r_s}{r}$ and

$$V_{eff}(r) = \left(1 - \frac{r_s}{r}\right)\left(\frac{l(l+1)}{r^2} + \frac{r_s}{r^3}\right). \tag{2.20}$$

The latter equation is an effective potential of the Schwarzschild BH. Note that it does not depend on the azimutal number m.

The equation (2.19) can be reduced to an equation with second-order derivatives only,

$$\left(\frac{\partial^2}{\partial r_*^2} - \frac{\partial^2}{\partial t^2} - V_{eff}\right) u_{lm}(t,r) = 0, \tag{2.21}$$

where r_* is so-called "tortoise coordinate" and can be obtained from the following relation

$$\frac{dr_*}{dr} = \left(1 - \frac{r_s}{r}\right)^{-1}.$$

The tortoise coordinate $r_* = r + r_s \ln\left(\frac{r}{r_s} - 1\right)$ approaches $-\infty$ as r approaches the Schwarzschild radius r_s and $+\infty$ as r approaches the spatial infinity.

It is convenient to separate variables in the u_{lm} function to factor time dependence out

$$u_{lm}(r,t) = e^{-i\omega t}\psi_{lm}(r) \tag{2.22}$$

and to obtain the stationary second-order equation

$$\left(\frac{d^2}{dr_*^2} + (\omega^2 - V_{\text{eff}}(r(r_*)))\right)\psi(r(r_*)) = 0 \tag{2.23}$$

which is formally equivalent to the one-dimensional Schrodinger equation for massive par-

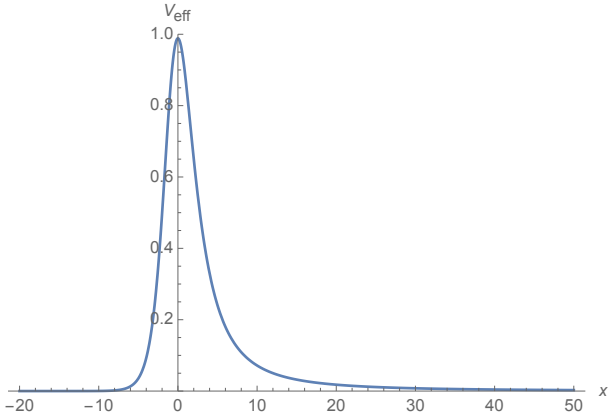

Figure 2.1: The graph of V_{eff} in the tortoise coordinate.

ticles with "energy" ω^2, where r_* varies from $-\infty$ to $+\infty$.

2.3 Linear gravitational perturbation

Pioneer's work in studying BH perturbation theory belonged to Regge and Wheeler [34] when they investigated the stability of the Schwarzschild BH in the middle of the past century. It was believed that the hypothetical BH was the last stage of a massive collapsed

star and therefore had to be stable under perturbation. The interest was that, in general, a solution to the Einstein equations does not imply the stability of a BH.

One method of stability analysis is to derive the first order approximations for the perturbation equations. This derivation is a linear equation which can be decomposed into normal modes using tensor spherical harmonics. Those oscillating modes have complex frequencies with positive and negative imaginary parts which indicate the stability or instability of a BH.

In this section, we summarize the main results obtained by Regge and Wheeler [34]. For a more detailed derivation, see the Appendix.

To derive the perturbed Einstein equation of a Schwarzschild BH, we first add the small term $h_{\mu\nu}$ to the metric tensor $g_{\mu\nu}$ such that total metric is the sum

$$\tilde{g}_{\mu\nu} = g_{\mu\nu} + h_{\mu\nu}, \quad |h_{\mu\nu}| << 1, \tag{2.24}$$

where $g_{\mu\nu}$ denotes the unperturbed metric (or background metric) shown in (2.10) in Schwarzschild coordinates. In perturbation theory, the background metric is only used to raise and lower the indices of $h_{\mu\nu}$

$$h^{\mu\nu} = g^{\mu\alpha} g^{b\nu} h_{\alpha\beta}. \tag{2.25}$$

Using this rule, we can write (2.24) with upper indices

$$\tilde{g}^{\mu\nu} = g^{\mu\nu} - h^{\mu\nu} + O(h^2) \tag{2.26}$$

To obtain the linearized form of Einstein equation in $h_{\mu\nu}$ term, we insert (2.24) and (2.26) in (2.2) beginning with the perturbed Cristoffel symbols (2.6), and then we calculate Ricci tensor and scalar given by (2.8) and (2.9)

$$\begin{aligned}
\tilde{\Gamma}^k_{\mu\nu} &= \frac{1}{2}\tilde{g}^{k\alpha}(\partial_\nu \tilde{g}_{\alpha\mu} + \partial_\mu \tilde{g}_{\alpha\nu} - \partial_\alpha \tilde{g}_{\mu\nu}) = \frac{1}{2}(g^{ka} - h^{ka})(\partial_\nu \tilde{g}_{\alpha\mu} + \partial_\mu \tilde{g}_{\alpha\nu} - \partial_\alpha \tilde{g}_{\mu\nu}) \\
&= \frac{1}{2} g^{ka}(\partial_\nu \tilde{g}_{\alpha\mu} + \partial_\mu \tilde{g}_{\alpha\nu} - \partial_\alpha \tilde{g}_{\mu\nu}) - \frac{1}{2} h^{ka}(\partial_\nu \tilde{g}_{\alpha\mu} + \partial_\mu \tilde{g}_{\alpha\nu} - \partial_\alpha \tilde{g}_{\mu\nu}) \\
&= \frac{1}{2} g^{k\alpha}(\partial_\nu g_{\alpha\mu} + \partial_\nu h_{\alpha\mu} + \partial_\mu g_{\alpha\nu} + \partial_\mu h_{\alpha\nu} - \partial_\alpha g_{\mu\nu} - \partial_\alpha h_{\mu\nu}) \\
&\quad -\frac{1}{2} h^{k\alpha}(\partial_\nu g_{\alpha\mu} + \partial_\nu h_{\alpha\mu} + \partial_\mu g_{\alpha\nu} + \partial_\mu h_{\alpha\nu} - \partial_\alpha g_{\mu\nu} - \partial_\alpha h_{\mu\nu}).
\end{aligned} \tag{2.27}$$

We rearrange terms in (2.27) and omit second-order $h\partial h$ terms and get

$$\begin{aligned}
\tilde{\Gamma}^k_{\mu\nu} = \frac{1}{2} g^{k\alpha}(\partial_\mu g_{\alpha\nu} + \partial_\nu g_{\alpha\mu} - \partial_\alpha g_{\nu\mu}) + \frac{1}{2} g^{k\alpha}(\partial_\mu h_{\alpha\nu} + \partial_\nu h_{\alpha\mu} - \partial_\alpha h_{\nu\mu}) \\
-\frac{1}{2} h^{k\alpha}(\partial_\mu g_{\alpha\nu} + \partial_\nu g_{\alpha\mu} - \partial_\alpha g_{\nu\mu}).
\end{aligned} \tag{2.28}$$

Then, the perturbed Cristoffel symbols have the following form

$$\tilde{\Gamma}^k_{\mu\nu} = \Gamma^k_{\mu\nu} + \delta\Gamma^k_{\mu\nu}, \tag{2.29}$$

where variation $\delta\Gamma^k_{\mu\nu}$ is

$$\delta\Gamma^k_{\mu\nu} = \frac{1}{2}g^{k\alpha}(\partial_\mu h_{\alpha\nu} + \partial_\nu h_{\alpha\mu} - \partial_\alpha h_{\mu\nu}) - g^{k\alpha}h_{b\alpha}\Gamma^b_{\mu\nu}. \tag{2.30}$$

Or, this formula might be re-written via the covariant derivative ";"

$$\delta\Gamma^k_{\mu\nu} = \frac{1}{2}g^{k\alpha}(h_{\alpha\nu;\mu} + h_{\alpha\mu;\nu} - h_{\mu\nu;\alpha}), \tag{2.31}$$

where the covariant derivative of two index tensor is

$$h^{\alpha\nu}_{;\mu} = h^{\alpha\nu}_{,\mu} + \Gamma^\alpha_{\sigma\mu}h^{\sigma\nu} + \Gamma^\nu_{\sigma\mu}h^{\alpha\sigma}, \tag{2.32}$$

with the comma sign denoting the standard derivative. The expression calculated for the Ricci tensor based on perturbed Cristoffel symbols derived before as

$$\tilde{R}_{\mu\nu} = R_{\mu\nu} + \delta R_{\mu\nu}, \tag{2.33}$$

where the variation of the Ricci tensor takes the form

$$\delta R_{\mu\nu} = \delta\Gamma^\alpha_{\mu\alpha;\nu} - \delta\Gamma^\alpha_{\mu\nu;\alpha}, \tag{2.34}$$

where the semicolon sign means the covariant derivative with respect to the metric (see (2.32)). As we study the perturbation of Einstein equations in a vacuum, the Ricci tensor has an unperturbed background metric equal to zero, $R_{\mu\nu} = 0$. Note that the perturbed space also has no matter.

So,

$$\delta R_{\mu\nu} = \delta\Gamma^\alpha_{\mu\alpha;\nu} - \delta\Gamma^\alpha_{\mu\nu;\alpha} = 0. \tag{2.35}$$

Due to spherical symmetry of BHs, the matrix of $h_{\mu\nu}$ will have the form (see [34])

$$h_{\mu\nu} = \begin{bmatrix} S & S & V_j \\ S & S & V_j \\ V_j & V_j & T_{kl} \end{bmatrix}.$$

The components $h_{tt}, h_{tr}, h_{rt}, h_{rr}$ transform as scalars and therefore can be constructed in the following way

$$S(t, r, \theta, \phi) = \sum_l \sum_{m=-l}^{l} h_{lm}(t, r)Y^m_l(\theta, \phi), \tag{2.36}$$

where Y_l^m are the spherical harmonics defined as

$$Y_{lm}(\theta,\phi) = \sqrt{\frac{2l+1}{4\pi}\frac{(l-m)!}{(l+m)!}}(-1)^m e^{im\phi} P_{lm}(cos\theta), \tag{2.37}$$

where $P_{lm}(cos\theta)$ are the associated Legendre functions of degree l and order m.

The components $h_{t\theta}, h_{t\phi}, h_{r\theta}, h_{r\phi}$ transform as vectors and have the following representations

$$(V^x_{lm})_\alpha = (S_{lm})_{;\alpha} = Y_{lm,\alpha},$$

$$(V^y_{lm})_\alpha = \epsilon^\nu_\alpha (S^m_l)_{;\alpha} = Y_{lm,\mu} = \gamma^{b\delta}\epsilon_{\alpha\delta} Y_{lm,b}.$$

Finally,the components $h_{\theta\theta}, h_{\theta\phi}, h_{\phi\theta}, h_{\phi\phi}$ transform as tensors and the expressions for them are given

$$(T^x_{lm})_{\alpha\beta} = Y_{lm;\alpha\beta},$$

$$(T^y_{lm})_{\alpha\beta} = \gamma_{\alpha\beta} Y_{lm},$$

$$(T^z_{lm}) = \frac{1}{2}\left(\epsilon^\nu_\alpha (T^x_{lm})_{\nu\delta} + \epsilon^\nu_b (T^x_{lm})\right) = \frac{1}{2}(\epsilon^\nu_\alpha Y_{lm;b\delta} + \epsilon^\nu_b Y_{lm;\alpha\delta}),$$

where indices α,b,ν run over values 2,3.

The matrix γ is the the metric tensor on the unit 2-sphere and ϵ is an anti-symmetric tensor. Note that all derivatives and tensorial operations we compute use the metric γ

$$\gamma_{\alpha\beta} = \begin{bmatrix} 1 & 0 \\ 0 & \sin^2\theta \end{bmatrix}$$

$$\epsilon_{\alpha\beta} = \sin\theta \begin{bmatrix} 0 & -1 \\ 1 & 0 \end{bmatrix}$$

2.4 Polar and axial perturbation

It turns out that the quantities introduced do not have the same parity. To clarify this we introduce the parity operator $\mathbf{P}$ that acts on some function $\psi(x)$ dependent on the following coordinates

$$\mathbf{P}\psi(x) = \psi(-x). \tag{2.38}$$

In our case the coordinate inversion is the inversion on a 2-sphere, which implies that the two families of parity are even (polar) and odd (axial). From tensor analysis, the tensor spherical harmonics are transformed as

$$\mathbf{P}(Y_{lm})_{\mu\nu} \to [\tilde{Y}_{lm}(\pi-\theta,\pi+\phi)]_{\mu\nu} \tag{2.39}$$

and behave in two distinct ways. In one case, the even parity harmonic acquires the factor of $(-1)^l$, while the odd parity harmonics have $(-1)^{l+1}$. The full analysis is written in the following papers [34], [31], [22].

We will emphasize that, while the rest quantities are polar, the V^y and T^z quantities are axial and multiplied by $(-1)^l$ under a parity transformation. This gives us the ability to study each separately by splitting $h_{\mu\nu}$ into two terms depending on parity

$$h_{\mu\nu} = h^{axial}_{\mu\nu} + h^{polar}_{\mu\nu}. \tag{2.40}$$

Following the analysis above, we compute the components of the axial $h^{axial}_{\mu\nu}$ part of the metric in the general form, given as where the functions W_{lm} and X_{lm} are defined as follows

$$h^{axial}_{\mu\nu} = \begin{bmatrix} 0 & 0 & -h_0(r,t)\sin^{-1}\theta\partial_\phi Y_{lm} & -h_0(r,t)\sin\theta\partial_\theta Y_{lm} \\ 0 & 0 & -h_1(r,t)\sin^{-1}\theta\partial_\phi Y_{lm} & -h_1(r,t)\sin\theta\partial_\theta \\ * & * & \frac{1}{2}h_2(r,t)\sin^{-1}\theta X_{lm} & -\frac{1}{2}h_2(r,t)\sin\theta W_{lm} \\ * & * & * & -\frac{1}{2}h_2(r,t)\sin\theta X_{lm}, \end{bmatrix},$$

$$\begin{aligned} X_{lm} &= 2(\partial_\theta\partial_\phi - \cot\theta\partial_\phi)Y_{lm}, \\ W_{lm} &= (\partial^2_\theta - \cot\partial_\theta - \sin^{-2}\theta\partial^2_\phi)Y_{lm}. \end{aligned} \tag{2.41}$$

Then we are free to choose a coordinate frame which best simplifies the axial metric. Here we rely on two facts. Firstly, that any coordinate frame is equivalent to any other if they are generally covariant, and, mapping one coordinate system to another is a differentiable bijection. Consider the coordinate transformation

$$x^{'\mu} = x^\mu - \eta^\mu$$

where we require η^μ to be infinitesimal, i.e. $\eta^\mu \ll x^\mu$ transforms like a vector quantity. Such transformation of coordinates implies the so-called gauge transformation of $h_{\mu\nu}$ as

$$h^{'}_{\mu\nu} = h_{\mu\nu} + \eta_{\mu;\nu} + \eta_{\nu;\mu}, \tag{2.42}$$

where the sum of last two terms form a gauge field. We note that such a transformation must decompose into spherical harmonics and observe parity invariance. For axial perturbation term of $h_{\mu\nu}$ as in the original paper we introduce the Regge-Wheeler gauge vector [34]

$$\eta^\mu = -\frac{1}{2}h_2(t,r)\cdot[0,0,\sin^{-1}\theta\partial_\phi,\sin\theta\partial_\theta]Y_{lm}. \tag{2.43}$$

Finally, the $h^{axial}_{\mu\nu}$ reduces to the form The last step towards obtaining the linearized Einstein equations reduced to (2.37) is the calculation of the components for the variation of the

$$h_{\mu\nu}^{axial} = \begin{bmatrix} 0 & 0 & -h_0(r,t)\sin^{-1}\theta\partial_\phi Y_{lm} & h_0(r,t)\sin\theta\partial_\theta Y_{lm} \\ * & 0 & -h_1(r,t)\sin^{-1}\theta\partial_\phi Y_{lm} & h_1(r,t)\sin\theta\partial_\theta Y_{lm} \\ * & * & 0 & 0 \\ * & * & * & 0 \end{bmatrix}.$$

Ricci tensor. The calculation shows that only three non-trivial differential equations with two unknown functions remain and are given as

$$\begin{aligned} A^{-1}(r)\partial_t h_0(r) - \partial_r(A(r)h_1(r)) = 0, \\ A^{-1}(r)(\partial_t^2 h_1(r) - \partial_{tr}^2 h_0(r) + \frac{2}{r}\partial_t h_0(r)) + \frac{1}{r^2}(l(l+1)-2)h_1(r) = 0, \\ \frac{1}{2}A(r)(\partial_r^2 h_0 - \partial_{tr}^2 h_1 - \frac{2}{r}\partial_t h_0) + \frac{1}{r^2}(r\partial_r A(r) - \frac{1}{2}l(l+1))h_0 = 0, \end{aligned} \tag{2.44}$$

where the function $A(r)$ is defined in eq.(2.23) see Ch.2.3.

Note that the two first equations reduce to the third one and thus, thanks to the successful choice of gauge, the entire analysis results in one equation. We will make an additional substitution of the function

$$Z^A = \frac{1}{r}A(r)h_1(t,r), \tag{2.45}$$

and express the time derivative of the first equation of (2.46) as

$$\partial_t h_0(t,r) = A(r)\partial_r(rZ^A), \tag{2.46}$$

we obtain the second order differential equation with only one unknown function

$$A(r)^{-1/2}\partial_{tt}^2(rZ^A) - \partial_r(rZ^A A(r)) + \frac{2}{r}A(r)\partial_r(rZ^A) + \frac{1}{r}[l(l+1)-2]Z^A = 0. \tag{2.47}$$

This equation takes the form of eq.(2.21) with similar effective potential as in Ch. 2.3. by introducing the "tortoise coordinate" (2.12) x

$$(\partial_t^2 - \partial_x^2 + V_{RW}(x))Z^A(x,t) = 0, \tag{2.48}$$

where the effective potential is called Regge-Wheeler potential and given as

$$V_{RW}(x) = \left(1 - \frac{r_s}{r(x)}\right)\left(\frac{l(l+1)}{r(x)^2} - \frac{3r_s}{r(x)^3}\right). \tag{2.49}$$

Note that, in the case of polar perturbations, the discussion is the same as for axial, and so the gauge vector is chosen as follows

$$\eta^\mu = [B_0(t,r), B_1(t,r), B(t,r)\partial_\theta, B(t,r)sin^{-2}\theta]Y_{lm} \tag{2.50}$$

where the functions B, B_0, B_1 are arbitrary and chosen to simplify the $h_{\mu\nu}^{polar}$. The procedure leads to the one-dimension wave equation which takes the same form as eq.(2.48)

$$(\partial_{tt}^2 - \partial_{xx}^2 + V_p(x))Z^P(t,x) = 0, \tag{2.51}$$

however the effective potential is a more complicated formula called the Zerilli potential

$$V_p(x) = A(r)\left(\frac{9r_s^3}{r^5\lambda^2} - \frac{3r_s^3}{2r^3\lambda^2}(l-1)(l+2)\left(1-\frac{3r_s}{2r}\right) + \frac{(l-1)(l+2)(l+1)l}{r^2\lambda}\right), \tag{2.52}$$

where $\lambda = l(l+1) + 3r_s/r - 2$. The two potentials V_p and V_{RW} (see Fig.2.2 below) have similar behaviour and decay exponentially at infinities.

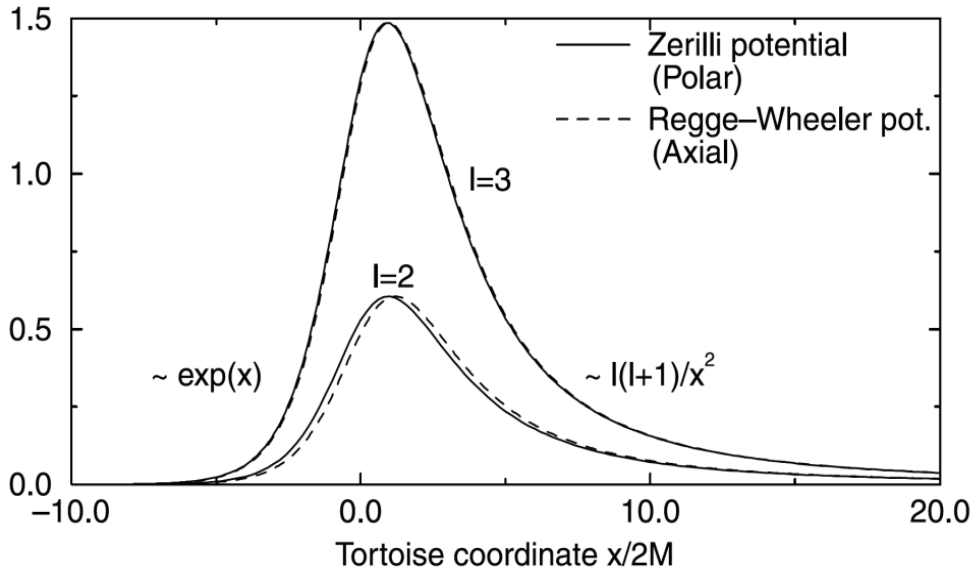

Figure 2.2: The graphs for the effective V_p(x) and V_{RW}(x) potentials for l=2 and l=3; From [31])

Chapter 3

Wormhole

3.1 History

In this chapter we turn to the second theoretical discovery made immediately after the creation of general relativity, namely the hypothetical existence of wormholes in the Universe. In 1916, the Austrian physicist Ludwig Flamm discovered a second solution to the Einstein's field equations (2.2) that exists in the Schwarzschild metric (2.10) called a white hole [26]. He argued that the solutions describing white and black holes in space-time are connected by a tunnel. In this hypothetical model, matter consumed by a BH ejects from a matching white hole. In 1935, Einstein and Rosen were the first to derive a wormhole

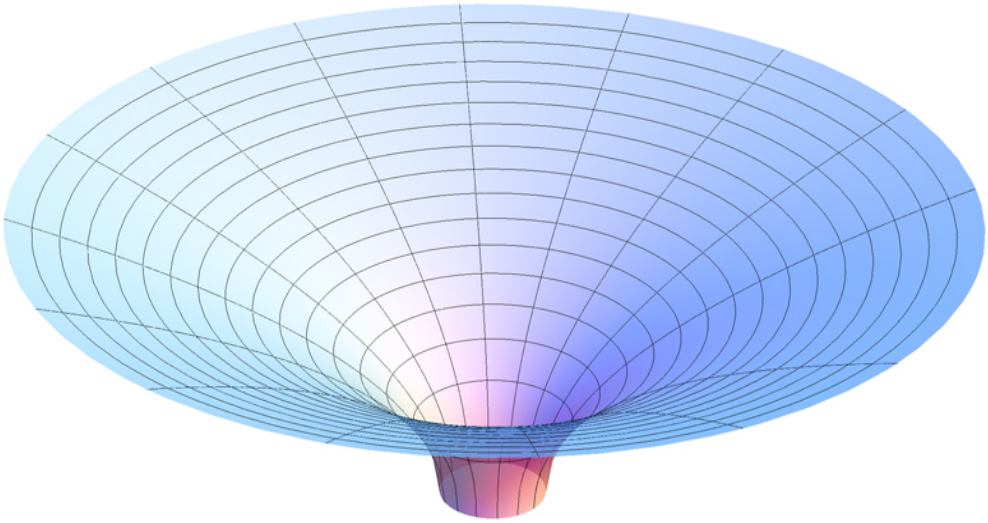

Figure 3.1: Flamm's parabaloid, see Article title: Schwarzschild metric - Wikipedia;

solution known as the Einstein-Rosen bridge [15]. The first modern concept and depiction of a WH was introduced into physics by the American physicist J.A. Wheeler in 1955. In 1957, in a well-known paper [29], Misner and Wheeler were the first to propose the term

wormhole for the general public. A basic wormhole can be represented as follows. There are two entrances to the wormhole (called **"mouths"** in the scientific literature [37]) which are connected by a "bridge" that lies outside of space-time. These mouths look like black holes, except WHs do not have an event horizon. If both WH mouths belong to one universe, it is labeled intra-universe, and inter-universe otherwise.

In 1973, Ellis and Bronnikov ([3],[17]) published results which demonstrated the theoretical existence of wormhole traversability in general relativity. Generally, a WH is "traversable" if a particle entering into a WH mouth can pass through the throat and exit from a WH or vice versa. The model of a wormhole proposed by Ellis was called the drainhole. A drainhole is a static, spherically symmetric solution of Einstein's field equations for a space-time vacuum with negative polarity that is minimally coupled to a scalar field.

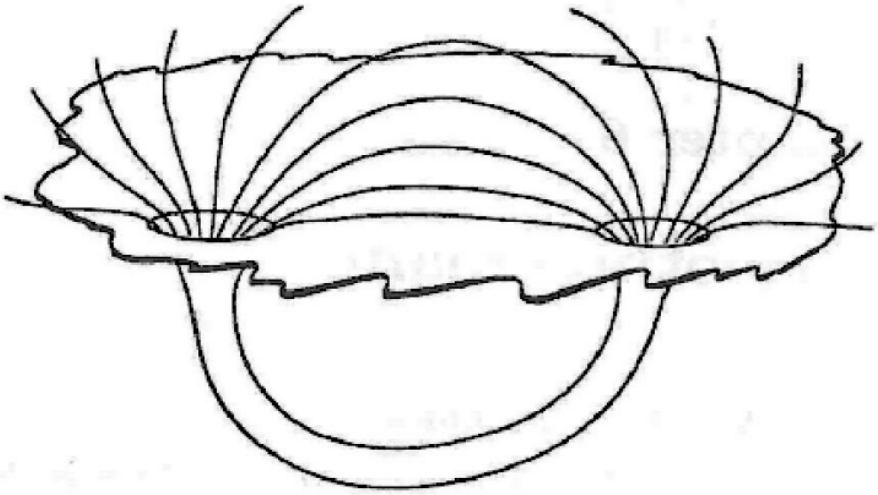

Figure 3.2: The first visual image of wormhole depicted by Wheeler in 1955. Note that a bridge (or a handle) lies outside of space-time; Taken from [39];

Wormholes are objects with a non-trivial topological structure (see Fig.3.4), the study of which has always been of considerable interest in general relativity. The physical laws require WHs to be empty, otherwise, under the influence of gravity, the bridge will collapse into a singularity. However, the existence of traversable wormholes require the presence of matter that violates a number of energy conditions to keep the mouths open and prevent a WH collapsing into a BH. This could be achieved by an exotic matter that has huge negative pressure to create anti-gravity, stabilizing the wormhole.

To date, there are arguments in favor that exotic matter of this kind can exist in the universe. This is due to the discovery of the Universe's accelerated expansion, which requires the introduction of a new substance, the so-called "dark energy", to explain. The hypothesis

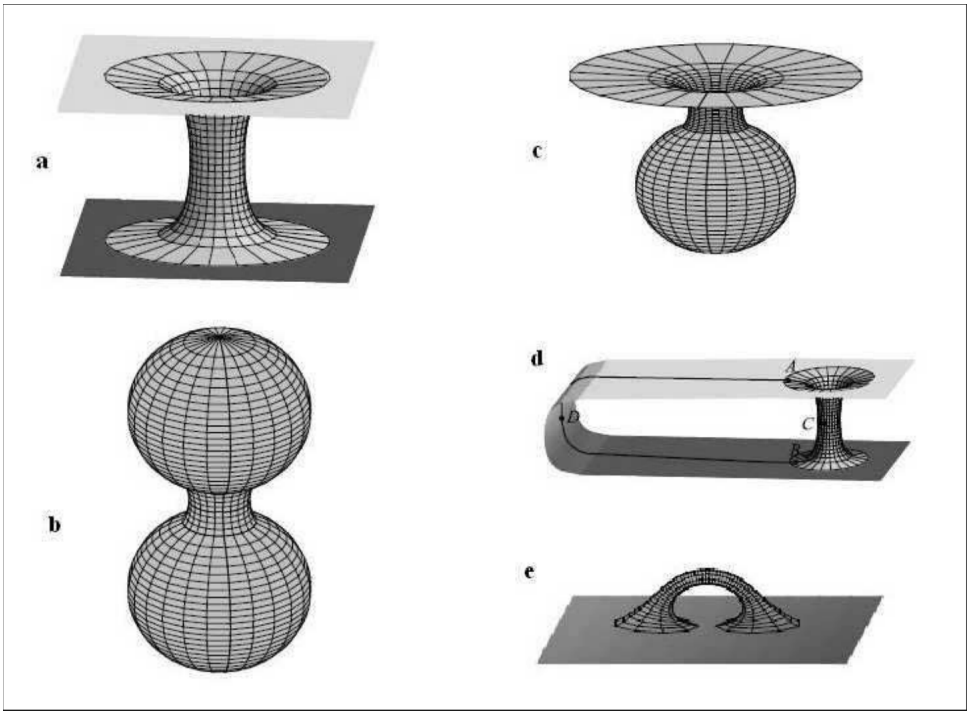

Figure 3.3: Different configurations of wormholes - two-dimensional analogues. Note that any wormhole has a bridge. The graph illustrates the following hypothetical types of WH. Wormhole obtained by connecting two flat spaces of different universes(a). A dumbbell-type space is a wormhole connecting two closed Friedman universes(b). The semi-closed world is a wormhole connecting Friedman's spherical closed universe with Minkowski space (c).Wormhole models with the bridge joins regions of same "universe"(d and e) (or a handle Image taken from [5])

of "dark energy" is supported by the study of the large-scale structure of the Universe, the anisotropy of the relic radiation, and estimates of the age and curvature of the Universe. According to modern estimates, our universe consists of 70% of "dark energy" (see, for example [13]).

While the origin of black holes is known and they have long been discovered in the universe, the origin of wormholes is debated, and there is no any evidence for their existence. Note that the outer parts of wormholes are very close to black holes. For this reason, a black hole can be indistinguishable for a wormhole when observed.

3.2 WH models

We consider the model called the Einstein-Rosen "neutral bridge". The term neutral means that there is no electrical charge associated with a WH. Starting from the Schwarzschild metric (2.10), we will make the coordinate transformation

$$u^2 = r - r_s,$$

so that $2udu = dr$ and $dr^2 = 4u^2du^2$, and the the new metric is

$$ds^2 = -\frac{u^2}{u^2+2M}dt^2 + 4(u^2+2M)du^2 + (u^2+2M)^2d\Omega^2, \tag{3.1}$$

with

$$u_{1,2}(r) = \pm\sqrt{r-r_s}. \tag{3.2}$$

The metric becomes an asymptotically flat at the limit of $u \to \pm\infty$. Two solutions of $u(r)$ are connected at the Scwarzschild radius by the hypersurface $u(r = r_s) = 0$. Einstein-Rosen bridge cannot be considered a traversable wormhole because these $u_{1,2}$ are two disconnected spacetimes which have one horizon and are nothing more than Schwarzschild wormholes and therefore have event horizon but not singularities.

In 1988, K. Thorne and M. Morris [30] proposed a concept of traversable spherically symmetric and static wormhole WH with pedagogical intentions to teach GR, they established criteria to make this traversal possible. In the GR, this wormhole should be a solution to the Einstein's field equations. This solution does not have any singularities as a WH has a throat which connects two asymptotically flat space-time regions.

Generally, the spherically symmetric static metric of such Morris - Thorne (MT) WH is given as

$$ds^2 = -f(r)^2dt^2 + \frac{dr^2}{1-\dfrac{b(r)}{r}} + r^2(d\theta^2 + \sin^2\theta d\phi^2), \tag{3.3}$$

where $b(r)$ is the wormhole shape factor and determines the spatial shape of the wormhole. The relation for the function $f(r)$ is given as

$$f(r) = e^{-\Phi(r)},$$

and $\Phi(r)$ is the red-shift function, responsible for describing how much the light bends in the gravitational background.

It is also useful to introduce the spatial coordinate associated with the proper frame of static observers. This coordinate l is defined as follows

$$dl^2 = \frac{dr^2}{1-\dfrac{b(r)}{r}}, \tag{3.4}$$

so that the MT WH metric (3.3) takes the form of :

$$ds^2 = -f(r(l))^2dt^2 + dl^2 + r(l)^2(d\theta^2 + \sin^2\theta d\phi^2), \tag{3.5}$$

with

$$l(r) = \pm\int_{r_0}^{r}\sqrt{1-\frac{b(r)}{r}}dr. \tag{3.6}$$

The function $\Phi(l)$ should be finite everywhere that implies an absence of event horizons - otherwise, a WH is non-traversable, the minimum of $r(l)$ corresponds to the point $l = 0$ and the area of a sphere at $l = const$ is $A(l) = 4\pi r^2(l)$. The condition for the existence of a throat is

$$\frac{dr(l=0)}{dl} = 0, \quad \frac{d^2r(l=0)}{dl^2} > 0, \tag{3.7}$$

and corresponds to a sphere with minimal area $A(0) = 4\pi r^2(0)$. The throat is understood as a space like two-dimensional closed surface Σ of minimal area.

The geometry of WH space-time is a priori four-dimensional therefore to better understand the geometric shape of WH the embedding diagram is used. The method consists of immersing the metric in a 3 dimensional Euclidean space. We consider the case of the static spherical symmetric wormhole the metric of which is given by formula (3.5).

The first step is to consider that the sketch takes place at a specific moment of time t and that we are working with a cross-section of the metric, namely, the following conditions are applied

$$t = const, \ \theta = \frac{\pi}{2}, \ dt = d\theta = 0.$$

Then the metric (3.3) has a form of

$$ds^2 = \frac{dr^2}{1 - \dfrac{b(r)}{r}} + r^2 d\phi^2. \tag{3.8}$$

The second step is to equate this metric to the metric of 3 dimensional euclidean space written in the cylindrical form

$$ds^2 = dz^2 + dr^2 + r^2 d\phi^2.$$

This will imply

$$\frac{dr^2}{1 - \dfrac{b(r)}{r}} + r^2 d\phi^2 = dz^2 + dr^2 + r^2 d\phi^2. \tag{3.9}$$

Expressing dz^2 via dr^2, we will get the differential equation which defines the shape of WH embedded in the 3 dimensional Euclidean space

$$\frac{dz(r)}{dr} = \pm \left(\frac{r}{b(r)} - 1 \right)^{-1/2}. \tag{3.10}$$

For the case of the Schwarzschild metric the $b(r) = r_s$ and by integrating (3.10)

$$z(r) = \pm \int \left(\frac{r}{r_s} - 1 \right)^{-1/2} dr, \tag{3.11}$$

we obtain the expression for the $z(r)$ function

$$z(r) = \pm 2\sqrt{r_s(r - r_s)} + C, \tag{3.12}$$

where C is the constant of integration.

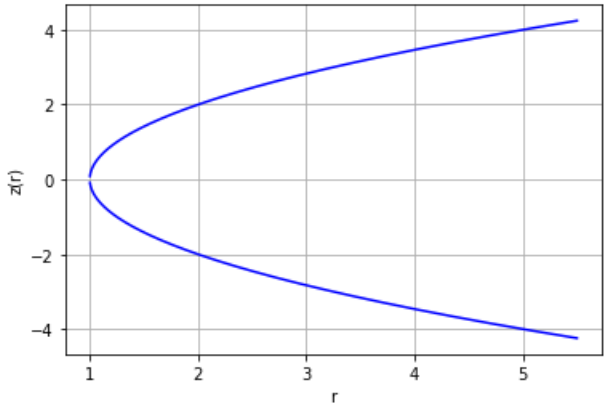

Figure 3.4: The graph (embedding diagram) of $z(r)$, which shows the shape of WH in Euclidean space.

Chapter 4

Quasinormal Modes of Schwarzschild Black Hole

4.1 Boundary conditions

In order to find the quasinormal modes and frequencies of the modes obeying the Eq.(2.21) we need to assign two boundary counditions to this equation. Notice that as "tortoise coordinate" r_* is approaching $\pm\infty$ the potential (2.20) vanishes and the equation reduces to the free wave equation

$$\Psi''(r_*) + \omega^2\Psi(r_*) = 0.$$

Then its solution can be written in the following form

$$\begin{cases} \Psi(r_*) = A_{out}e^{i\omega r_*} + A_{in}e^{-i\omega r_*}, \text{ as } r_* \to +\infty \ (r \to +\infty), \\ \Psi(r_*) = B_{in}e^{i\omega r_*} + B_{out}e^{-i\omega r_*}, \text{ as } r_* \to -\infty \ (r \to r_s), \end{cases} \tag{4.1}$$

where a negative sign in the exponents corresponds to the waves moving in the opposite direction of r_*-axis and otherwise for a positive one. Correct boundary conditions depend on what the physics problem we are studying. We focus on the time evolution of the BH perturbation caused by some external field or matter far from a BH therefore it is reasonably to assume that all radiation emitted is being carried away at large distance,i.e at spatial infinity, without further back scattering. Thus, A_{in} is zero to exclude the ingoing wave at $r \to +\infty$. We use the fact that nothing can escape the BH event horizon and then the outgoing wave exists at the horizon which corresponds to negative infinity in the "tortoise" coordinate, i.e. $B_{in} = 0$.

The boundary conditions are reduced to purely ingoing wave at the event horizon and purely outgoing wave at $+\infty$.

$$\begin{cases} \Psi(r_*) \propto e^{i\omega r_*}, \text{ as } r_* \to +\infty \\ \Psi(r_*) \propto e^{-i\omega r_*}, \text{ as } r_* \to -\infty \end{cases} . \tag{4.2}$$

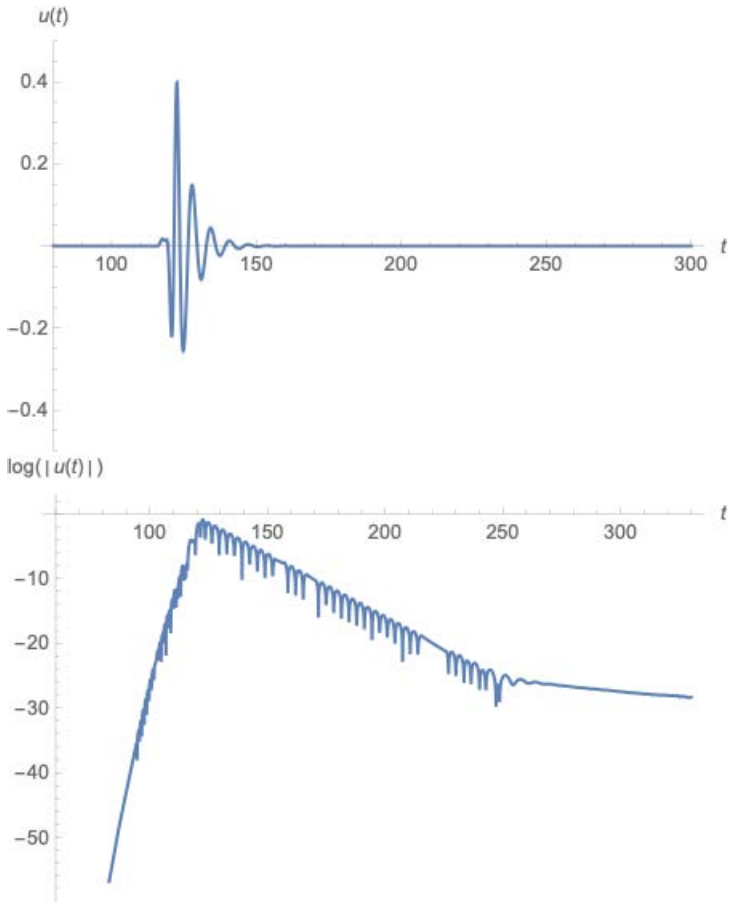

Figure 4.1: Time evolution of Schwarzschild BH perturbation caused by a scalar field for l = 2 localized at $r_* = 80r_s$ and plotted in linear and logarithmic coordinates. Remarkably, that the signal is damped by a characteristic ringing.

Using the Wolfram Mathematica we solve the problem for finding QNMs. As the initial condition at $t = 0$ we choose Gaussian wavepacket with the amplitude of $A = 30$ and $x_0 = 20$.

$$u_{20}^{scalar}(x,0) = Aexp\left(-\frac{x-x_0}{2\sigma^2}\right), \quad \partial_t u_{20}^{scalar} = \partial_x u_{20}^{scalar}(x,0), \quad u(t<0,x) = 0. \tag{4.3}$$

By looking at the graph plotted in absolute scale we can see that after the scattering of massless scalar field by BH, the Schwarzscild spacetime produces oscillations. These oscillations can be considered in different stages. First of all, the signal begins with a sharp transient emitted directly from the perturbation source which observer detects. Then, there is a stage of so-called QNMs ringing that are the oscillations with the decreasing amplitude. It can be seen that these QNMs last during the limited amount of time and have no asymptotic behaviour, however, they decay as tail at the late time, which is clearly visible in graph in logarithmic scale.

4.2 Quasinormal Frequencies

In this section, we would like to focus on the frequency spectrum of QNMs. First of all, let us consider again an initial left-moving toward a BH Gaussian wavepacket located at "infinite" distance from the event horizon of BH. Then in the Fourier space it will be given

$$u_0(t,x) = \int_{-\infty}^{+\infty} \frac{d\omega}{2\pi} A_{in}(\omega) e^{-i\omega t} e^{-i\omega x}, \tag{4.4}$$

where we supress subscript lm for u_{lm}, x is "tortoise coordinate" r_* and A_{in} is the amplitude of the initial wavepacket. We highlight the dependence of the amplitude on a frequency.

As we know from quantum mechanics (QM) that this causes scattering of wavepacket and we observe transmitted, left-moving, at $-\infty$ and reflected,right-moving, at $+\infty$ plane waves and they are given as follows

$$u_t(t,x) = \int_{-\infty}^{+\infty} \frac{d\omega}{2\pi} A_r(\omega) e^{-i\omega t} e^{-i\omega x}, x \to -\infty \tag{4.5}$$

$$u_r(t,x) = \int_{-\infty}^{+\infty} \frac{d\omega}{2\pi} A_t(\omega) e^{-i\omega t} e^{+i\omega x}, \quad x \to +\infty. \tag{4.6}$$

Then the asymptotic time-independent solution of (2.23) at $x \to +\infty$ is the superposition of (4.5) and (4.6) as both satisfy the (2.23)

$$u(t,x) = u_0(t,x) + u_r(t,x), \tag{4.7}$$

which after inserting in (2.23) will give

$$u(\omega,x) \approx A_0(\omega) e^{-i\omega x} + A_r(\omega) e^{+i\omega x}, \tag{4.8}$$

and the solution at $x \to -\infty$

$$u(\omega,x) \approx A_t(\omega) e^{-i\omega x}. \tag{4.9}$$

Returning to the QM course we apply the conservation law for probability which requires that the square of the amplitude of an incident wave is equal to sum of the squares of reflected and transmitted waves

$$|A_0(\omega)|^2 = |A_r(\omega)|^2 + |A_t(\omega)|^2, \tag{4.10}$$

Also, the amplitude for the reflection as know as reflection coefficient in QM is defined as

$$S(\omega) = \frac{A_r(\omega)}{A_0(\omega)}. \tag{4.11}$$

In the previous section we set the boundary conditions (4.2) such that there only purely outgoing waves at infinities after scattering due to the feature of the BH event horizon. It implies that $A_0(\omega)$=0 in the relation (4.11) with $A_r(\omega) \neq 0$. It breaks the conservation law for probability and leads to poles of scattering amplitute $S(\omega)$ and implies that there is no stationary perturbations.

We will write QNMs frequencies as

$$\omega = \omega_R + i\omega_I, \tag{4.12}$$

where ω_I must be negative for stability of the solutions and serves as resonances of the system. The question of stability of QNMs was studied at [10]. The numerical and analytical methods for extraction of the black hole quasinormal spectrum and solution are discussed in the next sections.

4.3 Third-order WKB approximation

In this subsection, we demonstrate one of the most popular semi-analytical method for computing values of quasinormal mode frequencies which is based on WKB approximation in quantum mechanics. This technique was introduced by Schutz and Will in 1985 (see [35]). It turns out that equation (2.23) is similar to one-dimensional stationary Schrodinger equation for a potential barrier. We begin with

$$\frac{d^2\Psi}{dx^2} + Q(\omega, x)\Psi = 0, \tag{4.13}$$

where $\mathrm{Q}(\omega, \mathrm{x}) = \omega^2 - \mathrm{V(x)}$ is a function of parameter ω and a coordinate x. We can consider ω as a quantum mechanical analog of particle's energy.

In our case, the physical meaning of Ψ is the radial factor of the perturbation variable, meanwhile the variable x is tortoise coordinate r_*, which ranges from $-\infty$ at the horizon to $+\infty$ at spatial infinity. The function V(x) is an effective potential of a black hole. In case of Kerr black hole an effective potential also depends on a spin parameter a. For the study we choose the Regge-Wheeler potential (see Figure 3.1) is

$$\mathrm{V}(r) = \left(1 - \frac{r_s}{r}\right)\left(\frac{l(l+1)}{r^2} + \frac{br_s}{r^3}\right),$$

where parameter l is an angular momentum index, b denotes $1 - s^2$, where s is a spin of perturbation, e.g. gravitational,scalar or electromagnetic. In order to get approximate solution (4.13), we modify this equation by introducing the small perturbation parameter ϵ, and write it down in the generic form:

$$\epsilon^2 \frac{d^2\Psi}{dx^2} + Q(\omega, x)\Psi = 0, \tag{4.14}$$

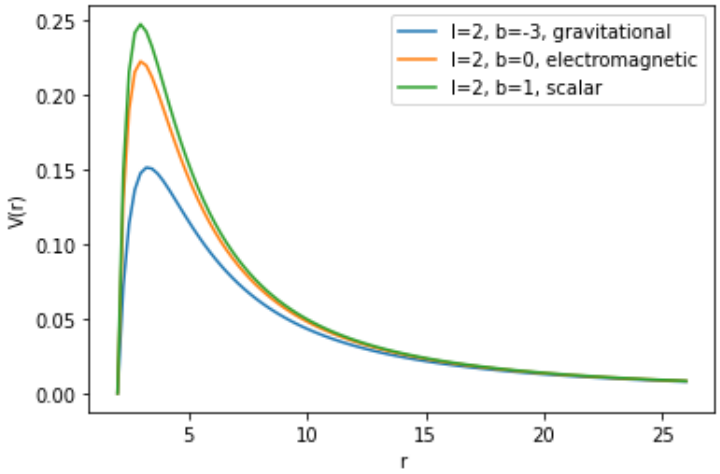

Figure 4.2: The graph of Regge-Wheeler potential for different types of perturbations.

We then approximate solution Ψ of this equation as the following ansatz:

$$\Psi = A \times \exp\left(\frac{S(x)}{\epsilon}\right), \tag{4.15}$$

where A denotes some amplitude and $S(x)$ is a power series expansion

$$S(x) = \Sigma_0^\infty \epsilon^n S_n(x), \tag{4.16}$$

Plug ansatz (4.15) with (4.16) in the equation (4.14), we get

$$\epsilon^2 \left(\frac{1}{\epsilon}\Sigma_0^\infty \epsilon^n S_n'(x) \cdot \exp\left(\frac{1}{\epsilon}\Sigma_0^\infty \epsilon^n S_n(x)\right)\right)' + Q(\omega, x)\frac{1}{\epsilon}\Sigma_0^\infty \epsilon^n S_n(x) = 0,$$

$$(\Sigma_0^\infty \epsilon^n S_n'(x))^2 + \epsilon \Sigma_0^\infty \epsilon^n S_n''(x)^2 + Q(x) = 0,$$

$$(S_0'(x)+\epsilon S_1'(x)+\epsilon^2 S_2'(x)+\epsilon^3 S_3'(x)+...)^2+(\epsilon S_0''+\epsilon^2 S_1(x)''+\epsilon^3 S_2(x)''+\epsilon^4 S_3(x)''+...)+Q(\omega,x)=0.$$

We need to equate the coefficients of powers of ϵ:

$$\epsilon : (S_0')^2 + Q(\omega, x) = 0,$$

$$\epsilon^2 : 2S_0'S_1' + S_0'' = 0,$$

$$\epsilon^3 : S_1'^2 + 2S_0'S_2' + S_1'' = 0.$$

The solution for S_0, S_1, S_2 can be obtained easily by integrating of those ordinary differential equations.

$$S_0(x) = \pm i \int^x \sqrt{Q(y)}dy,$$

$$S_1(x) = -\frac{1}{4}\ln Q(x),$$

$$S_2(x) = \mp\frac{i}{8}\int^x \left(\frac{Q''}{Q^{3/2}} - \frac{5}{4}\frac{Q'^2}{Q^{5/2}}\right) dy.$$

Therefore

$$S(x) = \pm i\int^x \sqrt{Q(y)}dy - \epsilon\frac{1}{4}\ln Q(x) + ...$$

That implies the wave function outside the effective potential

$$\Psi_1 = C_1 Q^{-1/4}\exp\left(\pm i\int_{x_2}^x \sqrt{Q(y)}dy\right), \Psi_3 = C_2 Q^{-1/4}\exp\left(\pm i\int_x^{x_1} \sqrt{Q(y)}dy\right)$$

We expand the expression for Q(ω,x) in a Taylor series around its maximum x_{max} to approximate solution of (4.13) in the region between two closely spaced turning points. Note here that the first derivative at maximum is zero.

$$Q(\omega, \mathrm{x}) = Q(\omega, \mathrm{x_{max}}) + \frac{1}{2}\frac{d^2Q(\omega, \mathrm{x_{max}})}{dx^2}(\mathrm{x} - \mathrm{x_{max}})^2 + o((\mathrm{x} - \mathrm{x_{max}})^3),$$

We just leave two first terms of the expansion for Q, by denoting $Q_0 = Q(\omega, \mathrm{x_{max}})$ and the second derivative at maximum as Q_0''.

$$\frac{d^2\Psi}{dx^2} + \left(Q_0 + \frac{1}{2}Q_0''(\mathrm{x} - \mathrm{x_{max}})^2\right)\Psi = 0,$$

Introduce the following function

$$k = \frac{1}{2}Q_0''$$

$$t = (4k)^{1/4}e^{i\pi/4}(x - x_0)$$

$$\nu + \frac{1}{2} = \frac{-iQ_0}{\sqrt{2Q_0''}} \tag{4.17}$$

Then the equation (4.13) takes the following form

$$\frac{d^2\Psi}{dx^2} + \left(\nu + \frac{1}{2} - \frac{1}{4}t^2\right)\Psi = 0$$

Therefore, the general solution of this equation is superposition of parabolic cylinder functions $D_\nu(t)$:

$$\Psi = AD_\nu(t) + BD_{-\nu-1}(it)$$

For large $|t|$ this solution has the following asymptotics (Bender and Orszag 1978),

$$\Psi \approx Be^{-3i\pi(\nu+1)/4}(4k)^{-(\nu+1)/4}(x - x_0)^{-(\nu+1)}e^{ik^{1/2}(x-x_0)^2/2} + [A + \frac{B(2\pi)^{1/2}e^{-i\nu\pi/2}}{\Gamma(\nu+1)}]\times$$

$$\times e^{i\pi\nu/4}(4k)^{\nu/4}(x-x_0)^{\nu}e^{-ik^{1/2}(x-x_0)^2/2}, \mathrm{x} \gg \mathrm{x}_2$$

$$\Psi \approx Ae^{-3i\pi\nu/4}(4k)^{\nu/4}(x-x_0)^{\nu}e^{-ik^{1/2}(x-x_0)^2/2}+\left(B-\frac{iA(2\pi)^{1/2}e^{-i\nu\pi/2}}{\Gamma(-\nu)}\right)e^{i\pi(\nu+1)/4}(4k)^{-(\nu+1)/4}\times$$

$$\times(x-x_0)^{-(\nu+1)}e^{ik^{1/2}(x-x_0)^2/2}, x \ll x_1,$$

where Γ is a gamma function in both solutions (see Apendix for more details). It can be seen that the requirement that Ψ is purely outgoing wave at spatial infinity in the formulas above can be reached by equating B and $\Gamma(-\nu)$ to zero and infinity correspondingly. The condition $\Gamma(-\nu) = \infty$ implies that ν mast be an integer. Then, from formula (4.17) we obtain

$$\frac{Q_0}{\sqrt{2Q_0''}} = i(n+\frac{1}{2}), \tag{4.18}$$

This is an quantum mechanical analog of so-called "Bohr–Sommerfeld quantization rule". It leads to descrete complex frequency spectrum by remembering that $\mathrm{Q}(\omega, \mathrm{x}) = \omega^2 - \mathrm{V(x)}$.

The location of maximum of $\mathrm{Q}(\omega, \mathrm{x})$ is defined from the relation of $(\omega^2 - V(x))' = 0$ which implies the quadratic equation

$$\lambda x^2 + 3(b-\lambda)x - 8b = 0,$$

where λ denotes $\mathrm{l(l+1)}$ and $GM = 1$.

It has two solutions and only positive one satisfies our goals

$$\mathrm{x}_{\max} = \frac{3}{2}\frac{\lambda - b + \sqrt{b^2 + (14/9)\lambda b + b^2}}{\lambda}.$$

The second-order derivative of $\mathrm{Q}(\omega, \mathrm{x})$ with respect to the coordinate is x.

$$Q''(x) = \left(1-\frac{2}{x}\right)\left(-\frac{\lambda}{x^4}\left(6-\frac{40}{x}+\frac{60}{x^2}\right)-\frac{2b}{x^5}\left(6-\frac{40}{x}+\frac{60}{x^2}\right)\right).$$

Now one can obtain quasinormal spectrum straightforwardly from equation (3.7).

In 1987, WKB approximation was extended to third order by Iyer and Will [20]. The relation (4.17) was corrected with two terms and has a form of

$$\frac{iQ_0}{\sqrt{2Q_0''}} - \Lambda(n) - \Omega(n) = n + \frac{1}{2}, \tag{4.19}$$

where

$$\Lambda(n) = \frac{1}{\sqrt{2Q_0''}}\left(\frac{1}{8}\left(\frac{Q_0^{(4)}}{Q_0''}\right)\left(\frac{1}{4}+\alpha^2\right)-\frac{1}{288}\left(\frac{Q_0'''}{Q_0''}\right)(7+60\alpha^2)\right), \tag{4.20}$$

and

$$\Omega(n) = \frac{n+\frac{1}{2}}{\sqrt{2Q_0''}}\left(\frac{5}{6912}\left(\frac{Q_0'''}{Q_0''}\right)^4(77+188\alpha^2) - \frac{1}{384}\left(\frac{Q_0'''^2 Q_0^{(4)}}{Q_0''^3}\right)(51+100\alpha^2)\right.$$
$$\left. + \frac{1}{2304}\left(\frac{Q_0^{(4)}}{Q_0''}\right)^2(67+68\alpha^2) + \frac{1}{288}\left(\frac{Q_0''' Q_0^{(5)}}{Q_0''^2}\right)(19+28\alpha^2) - \frac{1}{288}\left(\frac{Q_0^{(6)}}{Q_0''}\right)(5+4\alpha^2)\right) \tag{4.21}$$

It can be seen that the formulas (4.19) and (4.20) involve the high-order derivatives of the effective potential at the maximum which leads to some symbolic complexity which was resolved by using Wolfram Mathematica. The results for different type of perturbations with $l = 2$ are presented in Table 4.1 below and plotted in Fig 4.3. It can be seen that that

Table 4.1: Quasinormal modes frequencies for $b = -3$ and l = 2

n	Re ω	Im ω
0	0.373162	-0.0892174
1	0.346017	-0.274915
2	0.302935	-0.471064
3	0.247462	-0.672898
4	0.178753	-0.878675

Table 4.2: Quasinormal modes frequencies for $b = 0$ and l = 2

n	Re ω	Im ω
0	0.24587	-0.0931059
1	0.211309	-0.295835
2	0.164302	-0.50908
3	0.101924	-0.725608
4	0.0223294	-0.946159

Table 4.3: Quasinormal modes frequencies for $b = 1$ and l = 2

n	Re ω	Im ω
0	0.24587	-0.0931059
1	0.211309	-0.295835
2	0.164302	-0.50908
3	0.101924	-0.725608
4	0.0223294	-0.946159

the real part of frequency decreases with increasing of number n, while the absolute value of the imaginary part grows.

4.4 Continued Fractions Method

Another method for computation of QNMs spectrum [25] was proposed by Leaver in 1985. In this section, we follow and repeat his method as known as continued fraction method (CFM) applied for the Schwarzschild BH. First, let us consider the perturbation function in the Fourier space

$$u_{lm}(t,r,\theta,\phi) = \frac{1}{2\pi}\int e^{-i\omega t}\sum \frac{1}{r}\psi_l(r,\omega)Y_{lm}(\theta,\phi)d\omega.$$

The equation we are dealing with is given as

$$r(r-1)\partial_{rr}\psi_l(r) + \partial_r\psi_l + \left(\frac{\omega^2 r^3}{r-1} - l(l+1) + \frac{b}{r}\right)\psi_l = 0, \tag{4.22}$$

The equation above is called the generalized spheroidal wave equation. There are two singular points in the domain of eq.(4.22), one is a regular at $r = 1$ and another is an irregular which correspond to the negative and positive infinity respectively in the "tortoise" coordinate.

The two linearly independent solution of eq.(4.22) can be constructed

$$\psi_1(r) = (r-1)^{-i\omega}\sum_{n=0}^{\infty} a_n(r-1)^n, \qquad \psi_2(r) = e^{i\omega r}r^{i\omega}\sum_{n=0}^{\infty} a_n r^{-n}. \tag{4.23}$$

which obey the boundary conditions (4.2). However each of them has issue with complex plane and therefore it is more profitable to construct general solution as a product of those

$$\psi_l = (r-1)^{-i\omega}r^{2i\omega}e^{i\omega(r-1)}\sum_{n=0}^{\infty} a_n\left(\frac{r-1}{r}\right)^n. \tag{4.24}$$

The series in the formula above converges for $r \in (1/2, +\infty)$.

Inserting the expression (4.24) in eq. (4.22) we obtain a three-term recurrence beginning with $a_0 = 1$:

$$\begin{aligned} a_0 a_1 + b_0 a_0 &= 0, \\ a_n a_{n+1} + b_n a_n + c_n a_{n-1} &= 0, n = 1, 2... \end{aligned} \tag{4.25}$$

The exact relations for coefficients were derived in the original paper and are presented as follow:

$$\begin{cases} a_n = n^2 + 2(1-i\omega) + 1 - 2i\omega, \\ b_n = -(2n^2 + 2(1-4i\omega)n - 8\omega^2 - 4i\omega + l(l+1) + b), \\ c_n = n^2 - 4i\omega n - 4\omega^2 + b - 1. \end{cases}$$

It turned out that the sum (4.25) of coefficients converges if the following the condition holds

$$\frac{a_{n+1}}{a_n} \to 1 \pm \frac{(-2i\omega)^{1/2}}{n^{1/2}} - \frac{2i\omega + \frac{3}{4}}{n} + ... \tag{4.26}$$

The negative sign in the expression (4.26) leads to uniform convergence of the series in the (4.24). This will be satisfied if the ω is the eigenvalue of (4.22) that is quasinormal frequency. Then the ratio for two consecutive terms a_n has a form of infinite fraction and is represented as

$$\frac{a_{n+1}}{a_n} = \cfrac{-c_{n+1}}{b_{n+1} - \cfrac{a_{n+1}c_{n+2}}{b_{n+2} - \cfrac{a_{n+2}c_{n+3}}{b_{n+3} - ...}}}. \tag{4.27}$$

The brief notation for the relation (4.27) is

$$\frac{a_{n+1}}{a_n} = \frac{-c_{n+1}}{b_{n+1}-} \frac{a_{n+1}c_{n+2}}{b_{n+2}-} \frac{a_{n+2}c_{n+3}}{b_{n+3}-}.... \tag{4.28}$$

In order to obtain the equation for the quasinormal frequencies we set n to be zero $n = 0$ and get two equations:

$$\frac{a_1}{a_0} = -\frac{b_0}{a_0} \tag{4.29}$$

$$\frac{a_1}{a_0} = \frac{-c_1}{b_1-} \frac{a_1c_2}{b_2-} \frac{a_2c_3}{b_3-}.... \tag{4.30}$$

The equation (4.29) is called $n = 0$ boundary condition, while eq.(4.30) play role of boundary condition at $n = \infty$. We combine, by noticing the similarity of left-hand sides, both of them and get the expression for quasinormal frequencies:

$$0 = b_0 - \frac{a_0c_1}{b_1-} \frac{a_1c_2}{b_2-} \frac{a_2c_3}{b_3-}.... \tag{4.31}$$

Eventually, we deal with the extracting of frequencies from the eq.(4.31) which is a complex numerical problem due to the form of equation and an infinite number of fractions. Followed by Leaver's analysis we invert n times the eq.(4.31) for the getting the equality between finite and infite continued fraction:

$$\left[b_n - \frac{a_{n-1}c_na_{n-2}c_{n-1}}{b_{n-1} - b_{n-2}} \cdots \frac{a_0c_1}{b_0}\right] = \left[\frac{a_nc_{n+1}a_{n+1}c_{n+2}}{b_{n+1} - b_{n+2}-} \cdot ..\right] \tag{4.32}$$

It is clear that any numerical algorithm should run the finite number of iterations. For that reason we must truncate the number n until we reach our goals. For our purposes, we use Wolfram Mathematica to obtain all values of QNFs needed.

Table 4.4: Quasinormal modes frequencies for $b = -3$ and l = 2 calculated using CFM

n	Re ω	Im ω
1	0.373672	-0.0889623
2	0.346711	-0.273915
3	0.301053	-0.478277
4	0.251505	-0.705148
5	0.207516	-0.946845
6	0.169299	-1.195608

4.5 Poschl-Teller approximation

In this section we consider the problem of QNMs where the effective potential is represented by Poschl-Teller potential (see [32]) which has similar shape as the Regge-Wheller or Zerilli potentials and given by a formula

$$V(x) = \frac{V_0}{\cosh^2\alpha(x - x_0)}.$$

The scattering problem of GWs for Poschl-Teller potential was studied and solved analytically (see [18]), furthermore, it was revealed that exponentially decaying potentials prevents from backscattering of GWs. We just point this potential serves as a model for some BH theories.

Another reason is to study this potential is that it decays exponentially . Let us consider the wave equation with Poschl-Teller potential (see 4.1 [2])

$$\frac{\partial^2\Psi}{\partial r_*^2} + \left(\omega^2 - \frac{V_0}{\cosh^2\alpha(r_* - r_0)}\right)\Psi = 0, \tag{4.33}$$

where r_0 is the point of a maximum, V_0 is the constant that determines the height of the potential and

$$\alpha = \sqrt{-\frac{1}{2V_0}V''_{r_*(r_0)}}$$

The solutions of this second-order differential equation along with boundaries conditions (BCs) described in (4.2) for a given frequency ω are called QNMs. We introduce the following independent variable $\xi^{-1} = 1 + e^{-2\alpha(r_* - r_0)}$ in order to get solution of eq.(4.33) along with BCs and after some transformations we obtain

$$\xi^2(1-\xi^2)\frac{\partial^2\Psi}{\partial\xi^2} - \xi(1-\xi)(2\xi-1)\frac{\partial\Psi}{\partial\xi} + \left(\frac{\omega^2}{4\alpha^2} - \frac{V_0}{\alpha^2}\xi(1-\xi)\right)\Psi = 0.$$

It is possible to reduce this equation to a standard hypergeometric equation by substituting $\Psi = (\xi(1-\xi))^{-i\omega/(2\alpha)} y$ and therefore

$$\xi(1-\xi)\partial_\xi^2 y + [c-(a+b+1)\xi]\partial_\xi y - aby = 0, \tag{4.34}$$

where the constants c, a, b are defined as follow

$$a, b = [\alpha \pm \sqrt{\alpha^2 - 4V_0} - 2i\omega]/(2\alpha) \text{ and } c = 1 - i\omega/\alpha.$$

The general solution of this equation is given as

$$\Psi = A\xi^{i\omega/(2\alpha)} F(a-c+1, b-c+1, 2-c, \xi) + B(\xi(1-\xi))^{-i\omega/(2\alpha)} F(a, b, c, \xi), \tag{4.35}$$

Taking into account the BCs for QNMs near at spatial infinities the following relations should be valid

$$1 - \xi \sim e^{-2\alpha(r_* - r_0)} \ (r_* \to +\infty) \text{ and } \xi \sim e^{2\alpha(r_* - r_0)} \ (r_* \to -\infty).$$

We discuss that the constant A in (4.35) has to be zeroed because of $\xi^{(i\omega/(2\alpha))} \sim e^{i\omega r_*}$ which is ingoing wave at the negative infinity (or outgoing wave at the event horizon). Note that the function $F(a, b, c, \xi \to 0)$ is non zero (see [38]). The behaviour of the second term in (4.35) at infinity studied at [38] or [2] leads us to the following QNF spectrum

$$\omega_n = \pm\sqrt{V_0 - \frac{\alpha^2}{4}} - i\alpha\left(n + \frac{1}{2}\right), \tag{4.36}$$

where n is the overtone number. Another approach for obtaining the formula of QNF spectrum via algebraic techniques of Lie algebra were given in [7].

To compute quasinormal modes frequencies of Eq.(4.33) by using Wolfram Mathematica we use the Asymptotic Iteration Method (AIM) and follow [11] and [12].

Firstly, let us consider the homogeneous linear second-order differential equation (4.32) with $r_0 = 0$ and $\alpha = 0$:

$$\frac{d^2\psi}{dx^2} + \left(\omega^2 - \frac{1}{2}\text{sech}^2 x\right)\psi = 0 \tag{4.37}$$

$$\Psi'' = \lambda_0(x)\Psi' + s_0(x)\Psi,$$

and make a substitution of $y = \tanh x$. This transform eq.(4.37) into the following one

$$\psi''_{yy} - \left(\frac{2y}{1-y^2}\right)\psi'_y + \left[\frac{\omega^2}{(1-y^2)^2} - \frac{1}{2(1-y^2)}\right]\psi = 0. \tag{4.38}$$

, where transformed function ψ depends on y and $-1 < y < 1$. The BCs transform as follows

$$\begin{cases} \psi \sim (1-y)^{-i\omega/2}, \text{ as } y \to 1, \\ \psi \sim (1+y)^{-i\omega/2}, \text{ as } y \to -1. \end{cases} \tag{4.39}$$

Then we build the function ψ to satisfy (4.39)

$$\psi = (1-y)^{-i\omega/2}(1+y)^{-i\omega/2}\phi, \tag{4.40}$$

and we obtain the equation to apply AIM (see Apendix for more details)

$$\phi''_{yy} = \frac{2y(1-i\omega)}{1-y^2}\phi' + \frac{1-2i\omega-2\omega^2}{2(1-y^2)}. \tag{4.41}$$

We assign

$$\lambda_0 = \frac{2y(1-i\omega)}{1-y^2} \quad \text{and} \quad s_0 = \frac{1-2i\omega-2\omega^2}{2(1-y^2)},$$

and using Wolfram Mathematica run the algorithm to exctract spectrum. It turned out that the QNF spectrum obeys the following formula

$$\omega_n = \pm\frac{1}{2} - i\left(n+\frac{1}{2}\right).$$

We solve scattering problem for the equation (4.37) with Poschl-Teller potential which is considered in the literature as an approximation of the Regge Wheeler potential. The initial perturbation is $\psi(x,0) = exp^{-(x-20)^2}$. We notice that the profile of the scattered scalar field in this problem repeats the profile obtained in Ch.4.1. Results lead us to the conclusion

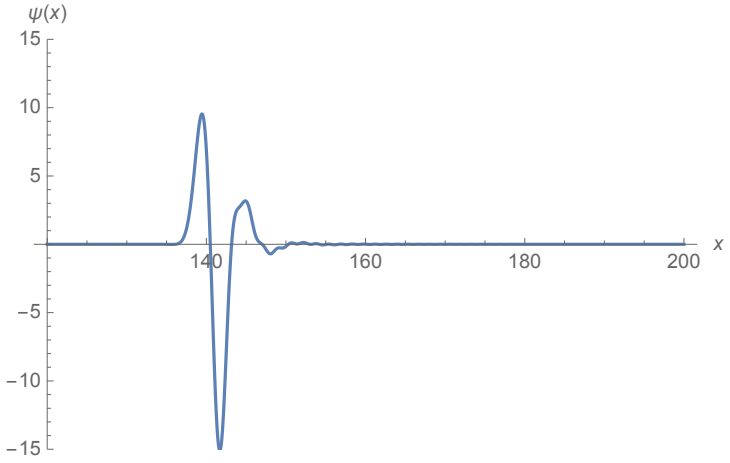

Figure 4.3: The graph of time evolution of perturbation of BH with Poschl-Teller potential caused by a scalar field $x = 20r_s$ plotted in linear.

that deviations from the Schwarzschild geometry of a black hole are pretty probable and

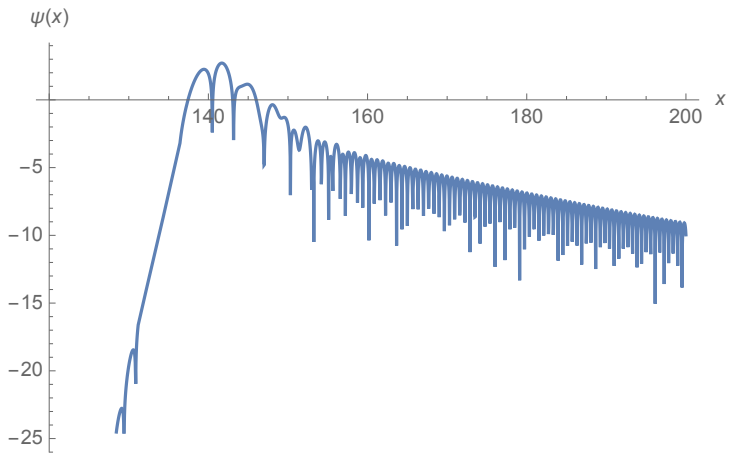

Figure 4.4: Scattered gaussian wavepacket plotted in logarithmic coordinates.There is a signal which is damped by a characteristic ringing.

require further study. Moreover, the scattered scalar fullness oscillates at entirely different frequencies.

Chapter 5

Echoes produced by Schwarzschild-like wormholes

5.1 Introduction

Observing BHs allows one to test gravity in a strong regime. However, a lot of uncertainty arises in measuring parameters of BHs. Therefore, the BH mimickers can be considered instead. In this chapter, we pay attention to popular exotic object as wormholes (WHs) which have been studied for the last decades. However, the boundary conditions for the horizonless objects differ from BH's ones and it was shown that these changes affect the picture of gravitational waves produced by WH. This phenomenon is related to the existence and properties of the photon sphere (light ring) around object [8], but if the WH geometry is close to a BH one, we expect to observe the ringdown phase ruled by QNMs. Therefore, this chapter aims to study WH's response in QNMs and identify the waveform features of different models. Furthermore, we are interested in the GWs emitted by a wormhole at late times due to a radially falling scalar field.

5.2 Ellis-Bronnikov wormholes

In this subsection, we give some revision [14] and study of the family of Ellis-Bronnikov (E-B) ([3],[17]) WHs of which we started discussion in Chapter 3.

The metric of E-B spacetime is given as

$$ds^2 = -dt^2 + \frac{dr^2}{1 - \frac{b_0^2}{r^2}} + r^2(d\theta^2 + sin^2\theta d\phi^2), \tag{5.1}$$

where b_0 usually plays role of throat radius.

It was shown that this metric reduces to the metric (3.3) and was given as the following relation

$$ds^2 = -dt^2 + dx^2 + r(x)^2(d\theta^2 + sin^2\theta d\phi^2) \tag{5.2}$$

where x is the proper radial coordinate.

As in Ch.2.2 (see eq.(2.16)) we want to derive the equation for scalar field $\phi(t, r, \theta, \phi)$ evolution on the background of (5.2) and repeat the procedure

$$\Box\phi = \sqrt{-g}\partial_\mu(\sqrt{-g}g^{\mu\nu}\partial_\nu)\phi = 0, \tag{5.3}$$

$$-\frac{\partial^2\phi}{\partial^2 t} + \frac{1}{r^2(x)}\frac{\partial}{\partial x}\left[r^2(x)\frac{\partial\phi}{\partial x}\right] + \frac{1}{r^2(x)}\left[\frac{1}{\tan\theta}\frac{\partial}{\partial\theta} + \frac{1}{\sin^2\theta}\frac{\partial^2}{\partial\phi^2}\right]\phi = 0 \tag{5.4}$$

and then decompose the function ϕ as the following

$$\phi \sim \frac{u_{lm}(x,t)}{r(x)}Y_{lm}(\theta,\varphi).$$

We note that the last term of (5.4) in the negative square brackets is square of the angular momentum operator which acts on spherical harmonics $Y_{lm}(\theta, \varphi)$ as follows

$$\hat{L}^2 Y_{lm}(\theta,\phi) = +l(l+1)Y_{lm}(\theta,\phi).$$

By making some transformation we obtain the following equation

$$\left(\frac{\partial^2}{\partial x^2} - \frac{\partial^2}{\partial t^2} - V_{eff}(r)\right)\Psi(x,t) = 0, \tag{5.5}$$

where the effective potential is given as

$$V_{eff}(r) = \frac{l(l+1)}{r^2(x)} + \frac{r''(x)}{r(x)}, \tag{5.6}$$

and where the prime means the coordinate derivative. Here we just focus on the specific family of WHs as known as Kar-Minwalla-Mishra-Sahdev (KMMS) [21] WHs for which the dependence of $r(x)$ is parameterized and given as

$$r^n(x) = (x^n + b_0^n), \tag{5.7}$$

where n is only even and $n >2$ and $x \in (-\infty, +\infty)$. The case of $n = 2$ is the EB WH.

$$V_{eff} = \frac{l(l+1)}{(b_0^n + x^n)^{2/n}} + \frac{(n-1)b_0^n l^{n-2}}{(b_0^n + x^n)^2} \tag{5.8}$$

Now we obtain QNMs on the background of KMMS wormholes with the exact the same boundary condition (see Ch.4) as it can be seen that the effective potential for such a family of WHs is a double barrier which can be naturally treated as two entrances of a WH. As we can see, there is a sharp transient as it was with Schwarzschild BH, which are then followed by QNM ringing. However, due to the form of potential the transmitted

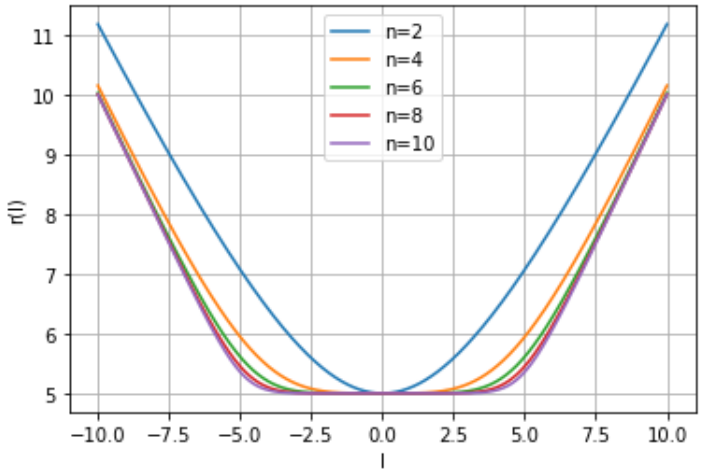

Figure 5.1: The dependence of r which is distance from the throat on proper coordinate x. We emphasize here that r run over only positive values while the proper coordinate varies from $-\infty$ to $+\infty$.

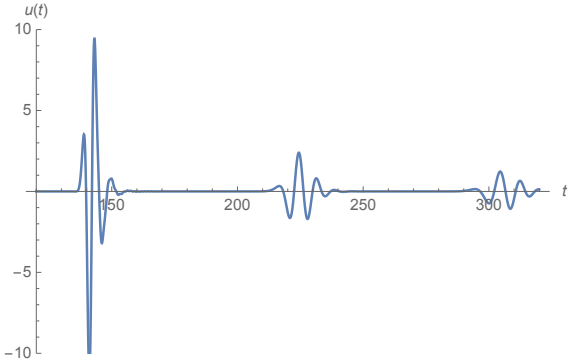

Figure 5.2: The series of echoes produced by the KMMS WH perturbed by a scalar field $\psi(x,0) = exp^{-(x-20)^2}$ with n=4 at x=100.

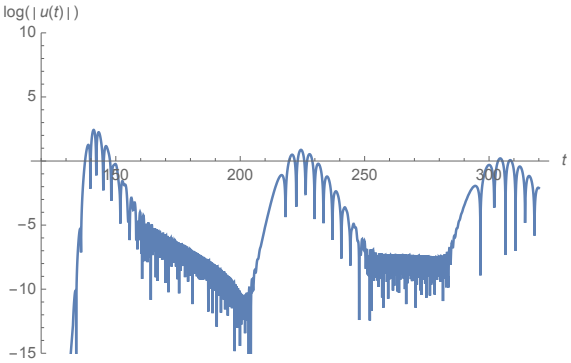

Figure 5.3: The initial QNM ringdown phase and repeated echoes with decreasing amplitude in semi-logarithmic scale.

wave experiences several reflections between potential walls. Therefore, subsequent signals arrive with a smaller amplitude of oscillations and are separated from each other by a finite time. The observed pattern is time-domain "echoes" which are emitted by a WH throat immediately after the initial signal. The detection of such echoes will allow refining the gravity theory model. We plotted the solutions in natural and semi-logarithmic scales for the scattering problem of the scalar field around WH geometry and can observe the echoes produced for different parameters.

5.3 Wormhole with double Poschl-Teller potential

In this subsection, we study the time evolution of scalar field in configuration of spherically symmetric traversable Morris-Thorne WH connected two infinities. This configuration is reached by the gluing of two identical Schwarzschild spacetimes at the throat where instead of Regge-Wheeler potential we use its approximation as Poschl-Teller potential (See Ch.3.A [6] and Fig.5.4) where we are free to vary the distance between two peaks. The double Poschl-Teller potential is given by the following formula

$$V(x) = \frac{V_0}{\cosh^2(x-a)} + \frac{V_0}{\cosh^2(x+a)}. \tag{5.9}$$

For the case of MT WH with double Regge-Wheeler see [4],[23]. It has been shown that WHs are ringing down qualitatively in the same way as black holes, unlike the latter they produce "periodic" recurring signals as known as "echoes" after the transient phase. The observation of those echoes during the Exotic Compact Objects (ECOs) coalesence will provide more information regarding the their existence and understanding their structure. It will shed light on the nature of processes in the strong gravity regime. Due to the inconsistency of quantum mechanics in the region of BH event horizon an alternative models i.e. horizonless objects for the study are considered. For the case of MT WH with double Regge-Wheeler see [19].

The boundary conditions are set to be the same as (4.2) in CH.4.1, therefore we apply a similar technique for finding QNMs. Meanwhile, the crucial difference from BH problem is that there is no horizon in WH case and no "tortoise" coordinates then. By looking at the

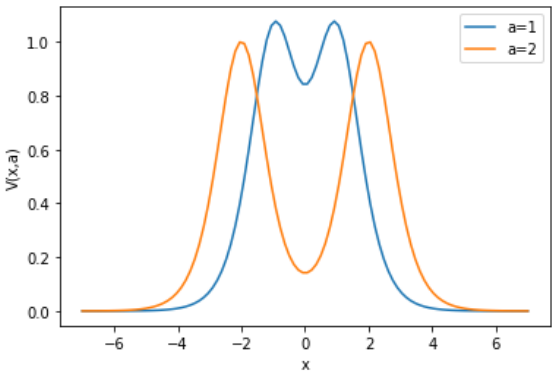

Figure 5.4: The picture for the effective potential (5.9) for a MT WH with. We see that the initial potential given in Ch.4.5 is bifurcated as the parameter a increases.

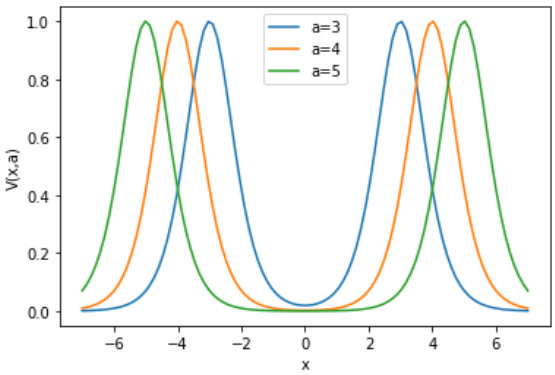

Figure 5.5: The picture for the effective double Poschl-Teller potential for the three diferent values of a. There is a strong separation of two bumps.

graphs, we see that with an increasing of parameter a we observe the appearance of clearly defined intermediate echo signals.In the semi-logarithmic scale, we notice that there is stage

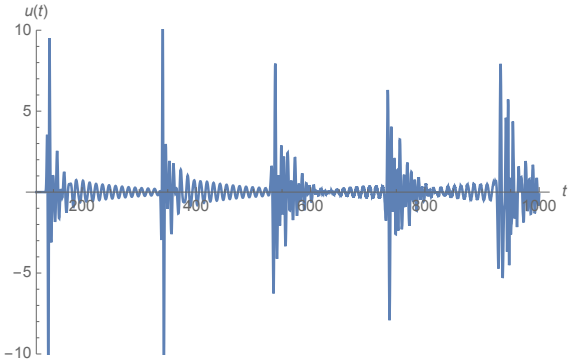

Figure 5.6: The WH response to a Gaussian wavepacket for $a = 3$ at $x = 100$. We see that WH produces the train of echoes.

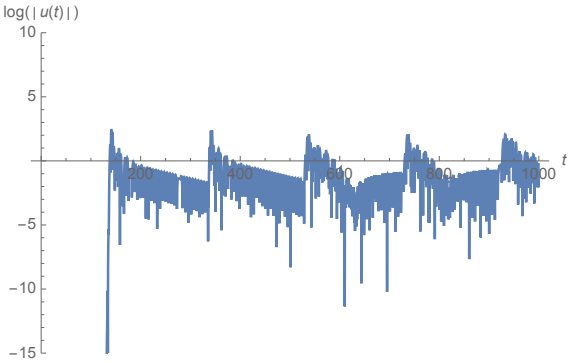

Figure 5.7: Scattered gaussian wavepacket $\psi(x, 0) = exp^{-(x-20)^2}$ for $a = 3$ at $x = 100$ plotted in semi-logarithmic scale.

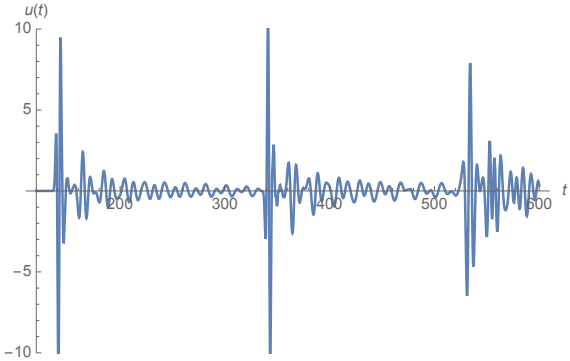

Figure 5.8: The WH response to a Gaussian wavepacket for $a = 5$ at $x = 100$.

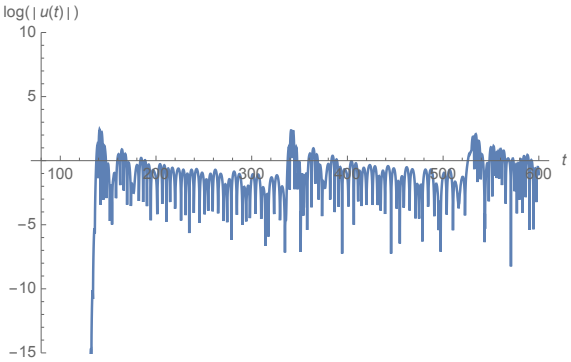

Figure 5.9: Scattered gaussian wavepacket $\psi(x, 0) = exp^{-(x-20)^2}$ for $a = 5$ at $x = 100$ plotted in semi-logarithmic scale.

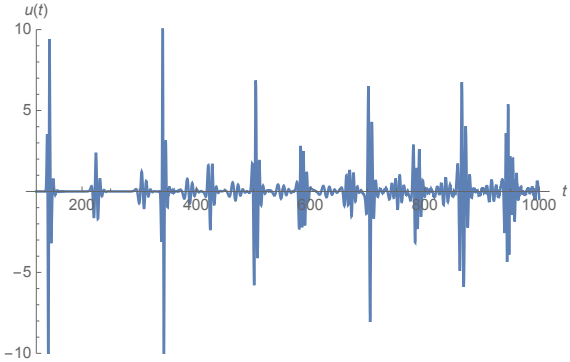

Figure 5.10: The WH response to a Gaussian wavepacket for $a = 20$ at $x = 100$.

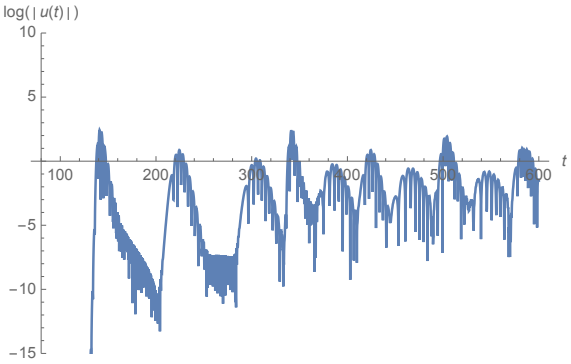

Figure 5.11: Scattered gaussian wavepacket $\psi(x, 0) = exp^{-(x-20)^2}$ for $a = 20$ at $x = 100$ plotted in semi-logarithmic scale.

of initial damped signal which was inherent to a BH response. However, we emphasize that later signal is a accompanied a train of echoes.

Chapter 6

Conclusion

This thesis studies the ringdown and late-time ringdown phases, the third phase of GW signal produced by two BH collided. These stages represent the most interest as they carry valuable information about the final product of the merger to study fundamental physics in the background of strong gravity. The GWs radiated by the new BH mathematically represented by the quasinormal modes oscillated at quasinormal frequencies (QNFs) related to them.

Instead of simulating two BHs colliding, we followed a different way. Precisely, we disturbed the Schwarzschild BH geometry by the scalar and gravitational field.

To analyze these processes theoretically, firstly, we derived the master equation for scalar perturbation. This is a non-homogeneous second-order wave equation where inhomogeneity is an effective potential barrier. Then, we formulated the scattering problem of the scalar field presented as a Gaussian wave-packet incoming toward the BH. This problem was solved, and the time evolution of the scalar field was plotted and analyzed using Wolfram Mathematica in Ch.2. The behaviour of this solution is damped oscillations with a power-law tail.

Secondly, we repeated the derivation of gravitational perturbations of Schwarzschild BH. In this case, we required Einstein's field equations to be linearized up to the first-order in perturbed metric terms. Remarkably, two types of these perturbations depend on the parity related to the rotation of the coordinate system. It turned out that in both cases, the master equations for the components of gravitational perturbation have the same form as in the scalar case. The different formulas gave the potential barriers, but they have similar behaviours and decay exponentially with time.

In Ch.4, we choose boundary conditions for the master equation by reasoning that the transmitted energy to the event horizon can not escape it and reflected radiation represents a purely outgoing wave. To extract the lowest QNFs associated with these oscillations, we applied numerical methods such as WKB, continued fraction method (CFM) and direct integration. We noted that the frequencies are complex numbers with negative imaginary parts. We also studied the behaviour of a scalar field against the background of a black hole

with another potential. The results show that the scattered wave profile similarly mimics the behaviour in Schwarzschild geometry. However, the frequency spectrum is radically different from that obtained in Chapter 2.

In the third chapter, we briefly overviewed the history of wormholes' development and pointed out their diversity. For example, although wormholes consist of two entrances and a bridge connecting them, one of the entrances geometrically repeats the appearance of a black hole. This fact led to an interest in studying the scattering of a scalar wave packet on a wormhole in the fifth chapter.

In Ch.5, we investigated the phenomenon of scattering a scalar wave packet on the background of a spherically symmetric static wormhole in a geometry similar to Schwarzschild's. Two models of wormholes were proposed for consideration, and we also studied the scattering of a scalar field in a toy model with a double Poschl-Teller potential. The motivation for the study was the reasonable question of how it is generally possible to distinguish between a black hole and a wormhole that externally have the same geometries. We have found that a wormhole produces an echo chain in all cases, which is not the case for a black hole at all. We conclude that with the advent of new detection technologies, it will be possible to determine whether we are receiving a signal from a pure black hole or a mole one.

A new series of astronomical observations is expected in the future, which will provide information for studying extreme compact objects and black holes. A comparison of the spectra will allow us to extract the parameters of these objects. However, due to the strong gravitational field, it is still unknown what geometry is very near the event horizon. Note, that the gravitational field (or curvature of space-time) is not necessarily very strong near the event horizon of astrophysical BHs (e.g. supermassive ones). In summary, the study of quasi-normal modes remains an important topic, if not a key one, for studying black hole physics and ECOs.

Bibliography

[1] B. P. Abbott et al. "Observation of Gravitational Waves from a Binary Black Hole Merger". In: *Phys. Rev. Lett.* 116 (6 Feb. 2016), p. 061102. DOI: 10.1103/PhysRevLett.116.061102. URL: https://link.aps.org/doi/10.1103/PhysRevLett.116.061102.

[2] Emanuele Berti, Vitor Cardoso, and Andrei O. Starinets. "Quasinormal modes of black holes and black branes". In: *Class. Quant. Grav.* 26 (2009), p. 163001. DOI: 10.1088/0264-9381/26/16/163001. arXiv: 0905.2975 [gr-qc].

[3] K. A. Bronnikov. "Scalar-tensor theory and scalar charge". In: *Acta Phys. Polon. B* 4 (1973), pp. 251–266.

[4] Kirill A. Bronnikov and Roman A. Konoplya. "Echoes in brane worlds: ringing at a black hole–wormhole transition". In: *Phys. Rev. D* 101.6 (2020), p. 064004. DOI: 10.1103/PhysRevD.101.064004. arXiv: 1912.05315 [gr-qc].

[5] Kirill A. Bronnikov and Sergey G. Rubin. *Black Holes, Cosmology and Extra Dimensions*. WSP, 2012. ISBN: 978-981-4374-20-0, 978-981-4440-02-8. DOI: 10.1142/8302.

[6] Pablo Bueno et al. "Echoes of Kerr-like wormholes". In: *Phys. Rev. D* 97.2 (2018), p. 024040. DOI: 10.1103/PhysRevD.97.024040. arXiv: 1711.00391 [gr-qc].

[7] A. F. Cardona and C. Molina. "Quasinormal modes of generalized Pöschl–Teller potentials". In: *Class. Quant. Grav.* 34.24 (2017), p. 245002. DOI: 10.1088/1361-6382/aa9428. arXiv: 1711.00479 [gr-qc].

[8] Vitor Cardoso, Edgardo Franzin, and Paolo Pani. "Is the gravitational-wave ringdown a probe of the event horizon?" In: *Phys. Rev. Lett.* 116.17 (2016). [Erratum: Phys.Rev.Lett. 117, 089902 (2016)], p. 171101. DOI: 10.1103/PhysRevLett.116.171101. arXiv: 1602.07309 [gr-qc].

[9] Sean Carroll. *Spacetime and Geometry: An Introduction to General Relativity*. Benjamin Cummings, 2003. ISBN: 0805387323. URL: http://www.amazon.com/Spacetime-Geometry-Introduction-General-Relativity/dp/0805387323.

[10] S. Chandrasekhar and Steven L. Detweiler. "The quasi-normal modes of the Schwarzschild black hole". In: *Proc. Roy. Soc. Lond. A* 344 (1975), pp. 441–452. DOI: 10.1098/rspa.1975.0112.

[11] H. T. Cho et al. “A New Approach to Black Hole Quasinormal Modes: A Review of the Asymptotic Iteration Method”. In: *Adv. Math. Phys.* 2012 (2012), p. 281705. DOI: 10.1155/2012/281705. arXiv: 1111.5024 [gr-qc].

[12] H. T. Cho et al. “Black hole quasinormal modes using the asymptotic iteration method”. In: *Class. Quant. Grav.* 27 (2010), p. 155004. DOI: 10.1088/0264-9381/27/15/155004. arXiv: 0912.2740 [gr-qc].

[13] Marek Demianski et al. “Investigating Dark Energy Equation of State With High Redshift Hubble Diagram”. In: *Front. Astron. Space Sci.* 7 (2020), p. 69. DOI: 10.3389/fspas.2020.521056. arXiv: 2010.05289 [astro-ph.CO].

[14] Poulami Dutta Roy, S. Aneesh, and Sayan Kar. “Revisiting a family of wormholes: geometry, matter, scalar quasinormal modes and echoes”. In: *Eur. Phys. J. C* 80.9 (2020), p. 850. DOI: 10.1140/epjc/s10052-020-8409-5. arXiv: 1910.08746 [gr-qc].

[15] A. Einstein and N. Rosen. “The Particle Problem in the General Theory of Relativity”. In: *Phys. Rev.* 48 (1 July 1935), pp. 73–77. DOI: 10.1103/PhysRev.48.73. URL: https://link.aps.org/doi/10.1103/PhysRev.48.73.

[16] Albert Einstein. “The Field Equations of Gravitation”. In: *Sitzungsber. Preuss. Akad. Wiss. Berlin (Math. Phys.)* 1915 (1915), pp. 844–847.

[17] H. G. Ellis. “Ether flow through a drainhole - a particle model in general relativity”. In: *J. Math. Phys.* 14 (1973), pp. 104–118. DOI: 10.1063/1.1666161.

[18] Valeria Ferrari and Bahram Mashhoon. “New approach to the quasinormal modes of a black hole”. In: *Phys. Rev. D* 30 (1984), pp. 295–304. DOI: 10.1103/PhysRevD.30.295.

[19] José T. Gálvez Ghersi, Andrei V. Frolov, and David A. Dobre. “Echoes from the scattering of wavepackets on wormholes”. In: *Class. Quant. Grav.* 36.13 (2019), p. 135006. DOI: 10.1088/1361-6382/ab23c8. arXiv: 1901.06625 [gr-qc].

[20] Sai Iyer. “BLACK HOLE NORMAL MODES: A WKB APPROACH. 2. SCHWARZSCHILD BLACK HOLES”. In: *Phys. Rev. D* 35 (1987), p. 3632. DOI: 10.1103/PhysRevD.35.3632.

[21] Sayan Kar et al. “Resonances in the transmission of massless scalar waves in a class of wormholes”. In: *Phys. Rev. D* 51 (1995), pp. 1632–1638. DOI: 10.1103/PhysRevD.51.1632.

[22] Kostas D. Kokkotas and Bernd G. Schmidt. “Quasinormal modes of stars and black holes”. In: *Living Rev. Rel.* 2 (1999), p. 2. DOI: 10.12942/lrr-1999-2. arXiv: gr-qc/9909058.

[23] R. A. Konoplya, Z. Stuchlık, and A. Zhidenko. "Echoes of compact objects: new physics near the surface and matter at a distance". In: *Phys. Rev. D* 99.2 (2019), p. 024007. DOI: 10.1103/PhysRevD.99.024007. arXiv: 1810.01295 [gr-qc].

[24] R. A. Konoplya and A. Zhidenko. "Quasinormal modes of black holes: From astrophysics to string theory". In: *Rev. Mod. Phys.* 83 (2011), pp. 793–836. DOI: 10.1103/RevModPhys.83.793. arXiv: 1102.4014 [gr-qc].

[25] E. W. Leaver. "An Analytic representation for the quasi normal modes of Kerr black holes". In: *Proc. Roy. Soc. Lond. A* 402 (1985), pp. 285–298. DOI: 10.1098/rspa.1985.0119.

[26] Francisco S. N. Lobo. "Introduction". In: *Fundam. Theor. Phys.* 189 (2017), pp. 1–7. DOI: 10.1007/978-3-319-55182-1_1.

[27] Michele Maggiore. *Gravitational Waves. Vol. 2: Astrophysics and Cosmology*. Oxford University Press, Mar. 2018. ISBN: 978-0-19-857089-9.

[28] Charles W. Misner, K. S. Thorne, and J. A. Wheeler. *Gravitation*. San Francisco: W. H. Freeman, 1973. ISBN: 978-0-7167-0344-0, 978-0-691-17779-3.

[29] Charles W. Misner and John A. Wheeler. "Classical physics as geometry: Gravitation, electromagnetism, unquantized charge, and mass as properties of curved empty space". In: *Annals Phys.* 2 (1957), pp. 525–603. DOI: 10.1016/0003-4916(57)90049-0.

[30] M. S. Morris, K. S. Thorne, and U. Yurtsever. "Wormholes, Time Machines, and the Weak Energy Condition". In: *Phys. Rev. Lett.* 61 (1988), pp. 1446–1449. DOI: 10.1103/PhysRevLett.61.1446.

[31] Hans-Peter Nollert. "TOPICAL REVIEW: Quasinormal modes: the characteristic 'sound' of black holes and neutron stars". In: *Class. Quant. Grav.* 16 (1999), R159–R216. DOI: 10.1088/0264-9381/16/12/201.

[32] G. Poschl and E. Teller. "Bemerkungen zur Quantenmechanik des anharmonischen Oszillators". In: *Z. Phys.* 83 (1933), pp. 143–151. DOI: 10.1007/BF01331132.

[33] Richard H. Price. "Nonspherical Perturbations of Relativistic Gravitational Collapse. II. Integer-Spin, Zero-Rest-Mass Fields". In: *Phys. Rev. D* 5 (1972), pp. 2439–2454. DOI: 10.1103/PhysRevD.5.2439.

[34] Tullio Regge and John A. Wheeler. "Stability of a Schwarzschild Singularity". In: *Phys. Rev.* 108 (4 Nov. 1957), pp. 1063–1069. DOI: 10.1103/PhysRev.108.1063. URL: https://link.aps.org/doi/10.1103/PhysRev.108.1063.

[35] Bernard F. Schutz and Clifford M. Will. "BLACK HOLE NORMAL MODES: A SEMIANALYTIC APPROACH". In: *Astrophys. J. Lett.* 291 (1985), pp. L33–L36. DOI: 10.1086/184453.

[36] Karl Schwarzschild. "On the gravitational field of a sphere of incompressible fluid according to Einstein's theory". In: *Sitzungsber. Preuss. Akad. Wiss. Berlin (Math. Phys.)* 1916 (1916), pp. 424–434. arXiv: physics/9912033.

[37] Matt Visser. *Lorentzian wormholes: From Einstein to Hawking*. 1995. ISBN: 978-1-56396-653-8.

[38] J. W. W. In: *Mathematics of Computation* 19.89 (1965), pp. 147–149. ISSN: 00255718, 10886842. URL: http://www.jstor.org/stable/2004114 (visited on 05/01/2022).

[39] J. A. Wheeler. "Geons". In: *Phys. Rev.* 97 (1955), pp. 511–536. DOI: 10.1103/PhysRev.97.511.